Published in final edited form as:
Parasitol Int. 2014 February ; 63(1): . doi:10.1016/j.parint.2013.09.013.

Imaging *Plasmodium* Immunobiology in Liver, Brain, and Lung

Ute Frevert[*], **Adéla Nacer**[&], **Mynthia Cabrera**[&], **Alexandru Movila**, and **Maike Leberl**[&]
Division of Medical Parasitology, Department of Microbiology, New York University School of Medicine, 341 E 25 Street, New York, NY 10010, USA

Abstract

Plasmodium falciparum malaria is responsible for the deaths of over half a million African children annually. Until a decade ago, dynamic analysis of the malaria parasite was limited to *in vitro* systems with the typical limitations associated with 2D monocultures or entirely artificial surfaces. Due to extremely low parasite densities, the liver was considered a black box in terms of *Plasmodium* sporozoite invasion, liver stage development, and merozoite release into the blood. Further, nothing was known about the behavior of blood stage parasites in organs such as brain where clinical signs manifest and the ensuing immune response of the host that may ultimately result in a fatal outcome. The advent of fluorescent parasites, advances in imaging technology, and availability of an ever-increasing number of cellular and molecular probes have helped illuminate many steps along the pathogenetic cascade of this deadly tropical parasite.

Introduction

Despite significant progress in battling malaria, *Plasmodium falciparum* is still responsible for 655,000 deaths annually, the vast majority of which occur in African children under 5 years of age [1]. While the initial round of replication of the parasite in the liver is clinically silent, the subsequent infection of red blood cells (RBC) results in various severe manifestations of the disease including cerebral malaria (CM) and acute lung infection/acute respiratory distress syndrome (ALI/ARDS). Because of the difficulty to monitor, at subcellular resolution, the pathogenesis of clinical malaria in infected patients' internal organs, various mouse models have been developed for intravital microscopy (IVM) to provide a better understanding of the basic biology of the parasite and the innate and adaptive immune responses of the host.

In this review, we focus on the considerable knowledge gained over the past decade on the dynamics of *Plasmodium* sporozoite entry into the liver, growth and maturation of the parasite's exoerythrocytic schizonts or liver stages (LS), the release of thousands of merozoites into the blood, the pathogenesis of experimental cerebral malaria (ECM), and the manifestation of malarial ALI/ARDS using high-resolution optical imaging approaches [2-4]. For a review on intravital observations of sporozoite transmission into the skin see the

[*]Corresponding author: Ute Frevert, Tel: 001-212-263-6755, Fax: 001-212-263-8116, ute.frevert@nyumc.org.
[&]Current addresses: Mynthia Cabrera: Department of Entomology, Pennsylvania State University, 548 Agricultural Sciences & Industries Building, University Park, PA 16802, USA. mxc92@psu.edu, Adéla Nacer: Biologie des Interactions Hôte-Parasite, Département de Parasitologie et Mycologie, Institut Pasteur, 25 rue du Docteur Roux, 75015 Paris, France. adela.nacer@pasteur.fr, Maike Leberl: University Colorado Anschutz Medical Campus, 12700 E 19 Ave, Aurora, CO 80045, USA. maike.leberl@ucdenver.edu

contribution of Jerome Vanderberg to this issue. While some of the IVM observations confirmed suspected events, others were completely unexpected. Thus, insight into the dynamics of cellular interactions is crucial as it will improve the design of subsequent studies aiming at characterizing the underlying molecular mechanisms.

1. Imaging the Elusive *Plasmodium* Liver Stage

Unlike any other organ in the body, the liver receives not only oxygenated arterial blood, but also nutrient-rich portal venous blood from the gastrointestinal tract [5, 6]. The two arterial and venous blood sources merge upon entry into the liver lobule and flow along the sinusoids towards the central venule. While the liver normally mounts an immune response against potential pathogens or toxins, it is typically tolerant to the large number of innocuous dietary and commensal antigens, microbial products and food antigens that arrive from the gastrointestinal tract via the portal venous blood [7, 8]. The liver harbors a resident population of professional macrophages, called Kupffer cells, which are crucially involved in the dichotomy between induction of tolerance or immunity [9].

1.1 Monitoring the hepatic microvasculature

Its unique metabolic and immunological features, combined with easy accessibility, have made the liver a major focus of IVM for many years [10, 11]. Due to its barrier function between the digestive system and the rest of the body, the liver is subject to a multitude of microbial infections. Monitoring microbial infection and the innate or acquired immune response of the host requires visualization of leukocytes infiltrating the hepatic microenvironment and their interaction with the various non-parenchymal antigen-presenting cells of the liver [9, 12]. IVM has provided insights into the regulation of the microcirculation of the liver and the function of Kupffer cells, the resident hepatic macrophages, in health and disease [13-19]. IVM also revealed differences in the molecular mechanisms underlying the recruitment of neutrophils and platelets during sepsis and sterile inflammation [20-25]. Further, liver IVM was used to visualize CXCR6+ NKT cells patrolling the hepatic sinusoids [26] and to characterize T cell and macrophage dynamics during mycobacterial granuloma formation [27, 28]. Finally, IVM proved a powerful tool to provide molecular information on intracellular signaling processes, cell division and death, cell migration and communication, as well as the *de novo* formation of microvascular blood networks during tumor progression and metastasis [29, 30].

1.2 Imaging the liver phase of the *Plasmodium* life cycle

After transmission by a female anopheline mosquito, *Plasmodium* sporozoites travel to the liver of the mammalian host, where they infect hepatocytes and grow rapidly to large LS [31]. Initial dynamic imaging studies of the *Plasmodium* infected liver focused on the basic biology of the parasite and mechanisms of survival in the hepatic microenvironment [2-4, 32, 33] (reviewed in [34]).

Some IVM observations confirmed suspected events. For example, sporozoite arrest and gliding along the sinusoidal endothelium [3] was expected based on a number of studies on the molecular interaction between the circumsporozoite protein of the parasite and extracellular matrix heparan sulfate proteoglycans of the liver [35-38]. Similarly, early digital IVM work using supported the notion that sporozoites use Kupffer cells as a gate to the liver after transmission by mosquito bite [3], which had been suspected based on various earlier studies conducted *in vitro*[36, 39, 40] and *in vivo*[41] (reviewed in [42, 43]). Electron microscopy revealed that in contrast to traversed hepatocytes [44], sporozoites enter a membrane-bound compartment of Kupffer cells without any obvious damage to the cell membrane of the macrophage [31, 36, 39, 45, 46], emphasizing the fundamental difference

between cells of epithelial versus phagocytic origin. *In vitro* studies suggest that this compartment is a non-fusogenic LAMP1-negative vacuole that allows the vast majority of WT sporozoites to persist inside Kupffer cells without evidence for loss of viability [39, 47], which is reminiscent of the ability of the evolutionarily older avian and reptilian Plasmodium species to live and multiply inside macrophages including Kupffer cells [48, 49]. These findings, together with the discovery that *P. yoelii* sporozoites are able to generate an anti-inflammatory cytokine secretion profile in Kupffer cells and to suppress the respiratory burst by interfering with the intracellular signaling pathways of these macrophages [50, 51], led to the hypothesis that *Plasmodium* may be able to exploit Kupffer cells as the port of entry into the liver [42, 52]. Ample evidence suggests that the macrophages emerge from encounters with sporozoites functionally crippled and moribund, destined to undergo programmed cell death [3, 39, 41, 47, 53-56].

A recent IVM study adds an important new dimension to the process of sporozoite entry into the liver. Tavares and coworkers showed that 23% of intravenously inoculated sporozoites crossed at a distance of Kupffer cells and without traversing an endothelial cell [47]. This phenotype is compatible either with a paracellular pathway between two endothelia or with a transcellular pathway through endothelia without loss of membrane integrity, for example by widening a pore within a sinusoidal sieve plate. This finding may explain the residual infectivity of SPECT-deficient parasites, which are completely cell traversal deficient [55] and prone to lysosomal degradation [47]. The majority of sporozoite crossing events (77%) occurred by cell traversal [47]. An elegant cytosolic fluorescence fading technique revealed that 16.7% of the sporozoite crossing events occurred by direct traversal of endothelial cells, without involvement of a Kupffer cell. An important outcome of the fading approach is that the endothelial cell membrane (like the membrane of traversed hepatocytes) is injured in the process of sporozoite traversal. A large proportion of the crossing events (36.6%) involved traversal of an endothelial cell after interactions with a Kupffer cell and 24% of the crossing events occurred by direct traversal of Kupffer cells, without involvement of endothelial cell traversal. Thus, ∼47% of cell traversal events involved both a Kupffer and an endothelial cell, while ∼53% of the sporozoites gained entry through a single cell type, an endothelial or a Kupffer cell. Sporozoite interactions with Kupffer cells were involved in ∼60% of all para- and transcellular crossing events, which corresponds to 78% of all cell traversal events. Thus, sporozoites could potentially exploit the tolerogenic properties of these resident macrophages of the liver [7-9, 57].

Interestingly, Kupffer cells are anchored to the sinusoidal wall by inserting a small footprint into the endothelial cell layer, while most of the cell body is located inside the sinusoidal lumen (reviewed in [57]). Based on this intricacy of the liver architecture, it seems possible that some parasites pass through the point of insertion of the Kupffer cell directly into the space of Disse, thus disabling only a Kupffer cell in the process. Those sporozoites that fail to exit Kupffer cells through the small footprint directly into the space of Disse, which is in fact rather likely, may subsequently traverse an underlying endothelial cell on their way into the liver. Interestingly, the endothelial and paracellular routes appear not to compensate for liver infection in the absence of Kupffer cells, because the liver burden of PyXNL sporozoite infected op/op mice was decreased by 84% compared to littermate controls with normal Kupffer cell numbers [41]. With the remote exception that op/op mice exhibit any resistance to *Plasmodium* LS development beyond their deficiency in macrophage-colony stimulating factor [58], these findings demonstrate that Kupffer cells are important for efficient sporozoite infection of the liver. This is of particular importance for natural infection conditions, where only minute numbers of parasites have been observed to reach the liver [3, 47]. In summary, the role of Kupffer cells as a major, although not exclusive, gate to the liver as well as the ability of the parasites to kill these phagocytes is now also clearly established *in vivo*[47]. Thus, all available evidence points towards sporozoites being

able to traverse a variety of cell types in a number of different tissues, an explanation that seems parsimonious and ties together the findings from different groups. As on many other occasions in the past, yet another level of complexity of the interaction between *Plasmodium* and the liver of the host has been uncovered. Improved purification techniques that minimize the amount of mosquito-derived cellular debris and microorganisms that typically contaminate sporozoite preparations while retaining parasite viability [59], combined with continued improvement of IVM techniques and instrumentation, are expected to further elucidate the mode and consequences of sporozoite traversal across the sinusoidal cell barrier.

IVM was used to monitor LS development in the livers of mice infected with *P. berghei* NK65 [3], *P. berghei* ANKA [2], and *P. yoelii* 17XNL [4, 32]. Comparison of the infection rates of fluorescent lines of these *Plasmodium* species/strains revealed the superiority of the *P. yoelii* 17XNL infected BALB/c mouse model for study of LS growth and biology, a crucial aspect considering the low number of parasites compared to the large mass of the liver and the limited surface area available for IVM observation. The asynchronicity of *Plasmodium* LS development further demands a high density of infected hepatocytes for collection of sufficient representative datasets per mouse for subsequent statistical analysis.

A series of elegant *in vitro* imaging studies, which offer the advantage of the defined 2D environment of hepatoma monocultures, has provided details on the mechanisms by which *Plasmodium* supports its survival in the liver. Imaging revealed that sporozoites undergo extensive metamorphosis after host cell invasion and that only organelles necessary for replication are retained [60]. In *P. berghei* infected Hepa 1-6 cells or *P. yoelii* infected HepG2-CD81 cells, host cell-derived cholesterol was shown to accumulate in the membrane of the parasitophorous vacuole surrounding the *Plasmodium* LS and documented the vacuole as a dynamic and highly permeable compartment with the ability to support the rapid growth of the intracellular parasite [61-63]. The *P. berghei* infected HepG2 cell model demonstrated the essential role of mitochondrial lipoic acid scavenging for *P. berghei* liver stage development [64], the reorganization of parasite and hepatocyte membranes during liver stage egress [65], the parasite-mediated inhibition of programmed death of its host cell [33, 66], and the involvement of a sporozoite-secreted cysteine protease inhibitor in hepatocyte invasion and prevention of host cell death [67]. *In vitro* live cell imaging also provided evidence for a verapamil-sensitive calcium channel in the membrane of *Plasmodium* LS, which contributes to changes in permeability of the parasitophorous vacuole membrane that precede the release of merozoites into the cytoplasm of the host cell [68]. The general cysteine protease inhibitor E64 was shown to block PV breakdown thus preventing merozoite liberation into the host cell cytosol [68].

Eventually, *Plasmodium* LS mature to thousands of merozoites, the stage of the parasite that infects erythrocytes and is responsible for the clinically symptomatic blood phase of the disease. Because merozoites have a short life span in the extracellular milieu and are highly susceptible to phagocytosis [69], the general assumption at the time was that merozoites, upon release from hepatocytes into the sinusoidal bloodstream, would immediately infect RBC to be able to safely bypass the gauntlet Kupffer cells on the way out of the liver. Surprisingly, however, IVM revealed that mature *P. yoelii* and *P. berghei* LS release merosomes, large membrane-bound structures containing hundreds of newly formed merozoites [2, 4, 32]. These large merosomes are shuttled out of the liver, down-sized while passing through the right heart, and arrested in the lungs, where they eventually release merozoites into the pulmonary microcirculation [4]. Interestingly, in the *P. berghei* HepG2 cell model, infected hepatoma cells detach from the culture vessel upon parasite maturation [2]. Although there is no direct *in vivo* correlate for this observation as hepatocytes are not expelled from the liver parenchyma upon merozoite release [4], HepG2 cell detachment *in*

vitro may reflect the separation of the hepatocyte membrane from the surrounding extracellular matrix *in vivo*, which is required to initiate the budding process associated with merosome formation [2, 4]. According to the current model, envelopment in a host-derived membrane that is characterized by low levels of the apoptotic marker phosphatidylserine allows hepatic merozoites to safely bypass the highly phagocytic Kupffer cells that line the liver sinusoids [2, 4, 41]. Merosome formation has therefore been likened a “Trojan horse” mechanism of immune evasion [65].

1.3 Technical aspects of intravital liver imaging

While early liver IVM work typically depended on transillumination microscopy and video recording, which restricted examination to the edge of the liver, the area of analysis was subsequently greatly extended by the use of wide-field epifluorescence microscopy [70-73]. Technical advances in instrument design over the years have to led to confocal, spinning disc, and 2-photon microscopes with vastly improved IVM and spectral capabilities [4, 10, 26-28, 74, 75]. Parameters such as sensitivity, image acquisition speed, Z-resolution, depth of analysis, phototoxicity and fluorochrome bleaching differ somewhat amongst the available equipment and it is up to the researcher to select an instrument capable of performing the specific task at hand.

Based on a decade of dynamic *in vivo* analyses of the liver, we consider the *P. yoelii* 17XNL infected BALB/c mouse, in particular the BALB/cAnNHsd strain, an excellent model for IVM based on its superior rate of LS development and negligible induction of unspecific inflammation [76, 77]. Stable transgene integration into the dispensable S1 (sporozoite expressed gene 1) locus of *P. yoelii*, which enables fluorescence expression throughout the parasite life cycle, has overcome the possibility of reversion by plasmid excision and also eliminated survival disadvantages associated with transgene expression in the small ribosomal subunit locus, a strategy previously utilized for both *P. berghei* and *P. yoelii*[32, 78]. The recent construction of powerful *P. berghei* strains such as luciferase-GFP, mCherry, tdTomato as well as novel GFP-expressing strains with improved brightness [79-83], in particular if used in combination with the wide range of transgenic or full knockout C57Bl/6 mice, which are more susceptible to *P. berghei*, should compensate for the higher levels of liver inflammation and the lower rates of LS maturation previously associated with this parasite.

The use of mice that were engineered to express fluorescence in certain cell types such as sinusoidal endothelial cells (Tie2-GFP), macrophages and neutrophils (lysM-EGFP), or dendritic cells (CD11c-YFP) and back-crossed into BALB/c background has aided in visualizing *P. yoelii* LS in the hepatic microenvironment [76, 84]. Mice expressing DsRed or CFP in all nucleated cells, for example, are useful for adoptive transfer of fluorescent T cells or bone marrow cells. Parasites that express fluorescent protein at all developmental stages are readily detectable in the liver tissue [32, 85], in particular if transfected with fluorochromes of improved photostability such as tdTomato and mCherry [81]. In contrast, LS from wild type (wt) parasites are inherently difficult to identify. As mosquitoes infected with wt parasites typically produce more oocysts in their midguts compared to those infected with fluorescent mutants, less time is spent on the tedious process of salivary gland dissection to collect the several million sporozoites necessary for intravital imaging. Therefore, methods were developed for identification of non-fluorescent parasites for cases in which fluorescent transgenic parasites are scarce or not available [76]. For example, DNA staining visualizes the hundreds of punctate merozoite nuclei that eventually fill the entire volume of mature LS and readily identifies the location of wt parasites in the liver parenchyma, especially if used in conjunction with transgenic mice such as Tie2-GFP mice or mice that express DsRed in all nucleated cells [76]. Another useful approach is to inject

the infected host with a mitochondrial stain, which provides structural details of the liver parenchyma and reveals the space occupied by non-fluorescent parasites [76].

The recent development of a novel microvascular imaging technique, termed intravital reflection recording (IRR), greatly improves visualization of the blood flow in non-fluorescent mice [76]. Based on simultaneous recording of reflected and autofluorescent signal, this approach visualizes plasma, blood cells, and the microvascular wall in the absence of fluorescent tracers. Recorded either in direct or inverse mode (Figure 1, Video S1 and Video S2), intravital reflection facilitates visualization of immune cells patrolling the sinusoidal microvasculature, adhering to the endothelium, and invading the parenchyma, and is thus ideally suited to monitor the response of the hepatic microenvironment to infection with *Plasmodium*. If used in combination with the multitude of cellular and molecular probes and reporter mice available, this method represents a powerful tool, because any laser line can be used to generate data in a complementary color, one major advantage of this technique [76]. There are many other potential applications of this novel imaging technique as well. For example, IRR will help identify up-regulation of endothelial surface molecules such as ICAM-1, CXCR6, or CD14 during vascular inflammation within selected sections of the microvasculature [26, 86, 87]. Because inverse IRR depicts (non-fluorescent) blood cells as bright objects on a dark background, this approach also eliminates the need for *ex vivo* labeling of erythrocytes for velocity measurements [71].

1.4 Interaction between *Plasmodium* liver stages and CD8+ effector T cells

Despite decades of research, *Plasmodium* LS still represent a major focus of antimalarial intervention and vaccine development [88-91], highlighting our incomplete understanding of the basic immunobiology of *Plasmodium* within the hepatic microenvironment. Vaccination with whole live radiation, genetically or chemically attenuated organisms, as well as viable parasites under drug cover, produces long-lasting sterile immunity in animal models [89, 92-97] and humans [90, 91, 98, 99]. Vaccination requires parasite invasion of the liver and, optimally, arrest at late stages of LS development [100]. Rodent malaria models suggest that CD8+ effector memory T cells play a central role in the elimination of *Plasmodium* infected hepatocytes from the liver [101-104]. Immunization with attenuated sporozoites generates a reservoir of hepatic CD8+ T cells, which is maintained by KC and DC derived IL-15 in the presence of a depot of parasite LS antigens, and that resident $CD44^{hi}CD45RB^{hi}CD122^{hi}CD62L^{lo/hi}$ CD8+ central memory T cells are required for the proliferation of IFN-γ producing $CD44^{hi}CD45RB^{lo}CD122^{lo}CD62L^{lo}$ effector memory T (T_{EM}) cells capable of conferring protection against reinfection [104-107]. *In vitro* studies have shown that *P. berghei* and *P. yoelii* specific CD8+ T cells are capable of contact-dependent recognition of parasite antigen on the surface of infected hepatocytes and elimination of LS in the absence of cytokines such as IFN-γ or TNF-α [108-110]. However, the cellular interactions and molecular effector mechanisms that lead to parasite killing *in vivo* are still poorly understood. Two recent studies have used IVM and adoptive transfer approaches to monitor the behavior of CD8+ effector/effector memory T cells in the liver [84, 111]. IRR was used to better visualize the dynamic events in the sinusoidal microvasculature surrounding *Plasmodium* LS to advance our understanding of the unique biology of this parasite in its natural hepatic microenvironment [76].

1.4.1 Behavior of splenic CD8+ effector T cells in the liver of infected mice—

Based on adoptive transfer of 9-10 million splenic *P. yoelii* CSP TCR transgenic CD8+ effector T cells into mice infected with 3×10^5 PyXNL sporozoites, Cockburn and coworkers monitored the behavior of the T cells in the vicinity of infected hepatocytes [111]. Although the average velocity of the CD8+ effector T cells was relatively low, suggesting that their ability to efficiently screen the liver was somewhat limited [112], the

study visualized for the first time CD8+ T cells killing *Plasmodium* LS following prolonged stable interactions with infected hepatocytes. Parasite death was associated with 4 different phenotypes: sudden loss of the bulk of the GFP signal, progressive attrition of parasite viability lasting hours, parasite blebbing, or complete loss of GFP signal in less than 5 minutes. Mathematical modeling as well as functional inhibition of G-protein coupled receptors with pertussis toxin revealed that clustering of the Py-specific CD8+ T cells around the infected hepatocytes and parasite elimination depend on a mechanism that involves positive feedback signaling mediated by GPCRs. Interestingly, antigen-unrelated OT-I CD8+ T cells moved at essentially the same velocity as the antigen-specific CD8+ effector T cells, both in the vicinity of and at a distance from infected hepatocytes [111], suggesting that the microenvironment of the entire liver, not only the neighborhood of infected hepatocytes, was altered in response to the infection. Thus, consistent with the notion that extraordinarily large frequencies of CD8+ effector T cells are required for sterilizing immunity [113], it appears that extreme numbers of CD8+ T cells must be present in the liver to allow detection of parasite antigen on infected hepatocytes.

1.4.2 Behavior of hepatic and splenic CD8+ effector memory T cells in the livers of naïve, immunized, and infected mice—Considering the important role of intrahepatic CD8+ T cells in protection, Cabrera and coworkers compared the behavior of hepatic and splenic CD8+ T_{EM} cells in the liver, both before and after adoptive transfer into sporozoite infected mice [84]. BALB/c mice were infected with 1-2 million PyXNL-GFP sporozoites and inoculated with 1 million fluorescent CD8+ T_{EM} cells isolated from the livers or spleens of Py-RAS, Pyuis4(-), or Pyfabb/f(-) sporozoite immunized mice. IRR was then used to monitor the behavior and location of the CD8+ T_{EM} cells with respect to the hepatic microvasculature (Figure 2, Video S2) [84]. Although CD8+ T cells were observed actively patrolling the livers of the immunized donor mice, neither hepatic nor splenic CD8+ T cells exhibited any significant velocity following adoptive transfer into infected or uninfected control mice. Despite variation of the timing of CD8+ T cell purification relative to challenge, adoptive T cell transfer relative to sporozoite inoculation, and IVM relative to infection and adoptive transfer, the CD8+ T_{EM} cells remained immotile for a period of at least 3 days after adoptive transfer. This loss of motility was observed for CD8+ T cells from donor mice immunized with Py-RAS, Pyuis4(-), or Pyfabb/f(-) sporozoites, as well as for Py-$CS_{280\text{-}288}$ epitope-specific TCR transgenic CD8+ T_{EM} cells [84]. Although the relatively high parasite density should have facilitated LS recognition, surprisingly none of the transferred hepatic or splenic CD8+ T cells approached or made contact with infected hepatocytes under any of the experimental conditions used in this study. The implications of these findings for immunity against malaria LS were recently discussed in the context of the hepatic blood lymph counterflow concept [114]. Many of the CD8+ T_{EM} cells from attenuated sporozoite-immunized mice, in particular those of splenic origin, were likely not parasite-specific, yet they were equally immotile in the liver after adoptive transfer [84]. This finding is reminiscent of the antigen-unrelated OT-1 in the Cockburn study, whose velocity equaled that of the Py-specific CD8+ T cells [111].

Jointly, these two complementary IVM studies suggest that CD8+ effector/effector memory T cells, whether of hepatic or splenic origin and whether parasite-specific or not, exhibit equally decreased velocity in the liver, both after adoptive transfer into infected and uninfected naïve control mice, but are nevertheless able to target infected hepatocytes via a GPCR-dependent mechanism and kill the intracellular parasites [84, 111]. Both studies represent a useful starting point for further refinement in the future.

1.5 Whole mouse imaging

While restricted in resolution and signal detection and thus not suitable for single cell analysis, detection of luminescence emitted by luciferase expressing parasites offers the distinct advantage that multiple readings can be collected from intact animals over long periods of time. For example, transgenic *P. berghei* GFP-luciferase (PbGFP-Luc_{CON}) parasites have provided important visual information on the parasite load in the liver and the overall state of protection of animals immunized with attenuated parasites [82, 83]. Whole mouse imaging is also a promising approach for screening antimalarial drugs directed against *Plasmodium* liver stages [115].

2. Imaging Cerebral Malaria Pathogenesis

Pediatric severe malaria is known to involve the accumulation of infected red blood cells (iRBC), monocytes, and platelets in the microvasculature of the central nervous system [116, 117]. Several other organs, in particular the lungs, are also involved (see below). Since more is known about the molecular and cellular events occurring in the brain, we review the pathogenesis of CM first. In fatal cases of human cerebral malaria (HCM), brain capillaries can be packed with pigmented iRBC [118-122]. According to a current model [116], HCM begins with the sequestration of iRBC to the microcirculation. The principal parasite ligand on the surface of human RBC infected with *P. falciparum* is the variant antigen PfEMP-1, encoded by the *var* gene family [117, 123, 124]. Its various adhesive domains mediate rosetting as well as adhesion to receptors on vascular endothelia of the host including ICAM-1, CD36, CD31, chondroitin sulfate A (CSA), and heparan sulfate [117]. Multiple mechanisms have been implicated in iRBC sequestration including direct adhesion to CD36 of the endothelial cell surface, indirect binding via platelet LFA-1 to endothelial ICAM-1, mechanical trapping of rosettes mediated by CD36 on platelets, and increased rigidity of the parasitized cells [125]. While no orthologues exist in other *Plasmodium* species, the *pir* superfamily, identified in rodent and human malaria parasites, has been implicated in cytoadherence, immune evasion, and antigenic variation [126].

Further parasite or host factors have been implicated in pathogenesis. For example, the local release of *Plasmodium* glycosylphosphatidylinositol during iRBC rupture is thought to induce an inflammatory acute phase response. Alternatively, the digestive vacuole membrane has been proposed as an inflammatory signal and it has been shown to trigger complement activation and clotting as well as promote fibrin formation in platelet-free plasma [127]. Further evidence implicating the digestive vacuole in pathology comes from the rodent *P. berghei* model, in which infection of mice with a parasite carrying a disrupted copy of the plasmepsin IV gene led to changes in both virulence and ECM. Specifically, susceptible mouse strains became resistant to ECM and ECM-resistant mice were able to clear the infection [128]. Platelets become activated by TNF-α and adhere directly to endothelial cells mediated by binding of CD40 to CD40 ligand (CD40L) [129, 130]. This early event appears to represent an important trigger for inflammation and tissue injury. Secretion of IL-1 from platelets may then lead to local endothelial activation with up-regulation of adhesion molecules such as ICAM-1 and production of cytokines such as IL-6 and chemokines that activate neutrophils and attract monocytes. After recognizing iRBC via pattern recognition receptors, monocytes differentiate to macrophages, become activated, produce reactive oxygen species (ROS) and secrete chemokines [131]. The ensuing endothelial damage attracts additional macrophages that interact with endothelia and platelets and further alter the function of the vascular endothelium. These inflammatory processes are thought to provide additional endothelial receptors for the sequestration of leukocytes that express P-selectin glycoprotein ligand 1 (PSGL1) and CD40 on their surface for binding to platelet selectin (P-selectin) and CD40L, respectively. While various leukocytes clearly contribute to the pathogenesis of ECM, liposome-encapsulated clodronate

elimination of macrophages did not prevent disease [132], CD8+ T cells are generally considered the terminal effector cells [133-136]. Eventually, after several rounds of amplification, the inflammatory cascade compromises the blood brain barrier (BBB) resulting in perivascular edema and hemorrhages, metabolic dysfunction, and neuronal injury. Ultimately, CM can lead to unrousable coma and death.

2.1 Imaging human cerebral malaria

Very few methods enable the monitoring of neuropathology in HCM patients. Computer tomography (CT) scans combined with ophthalmic examination including follow-up CT scans 7-18 months later have confirmed some of the pathological changes in the brains of pediatric patients (e.g. edema, herniation, ventricular changes) and the extent of 'recovery' following a CM episode [137]. Recently, magnetic resonance imaging (MRI) of pediatric cerebral malaria patients has become available in Blantyre, Malawi [138] and has provided some insights into macroscopic neuronal changes associated with pathology [137]. Although a wide range of changes was reported, some were correlated to retinopathy with involvement of the basal ganglia being the most common finding, followed by increased brain volume with herniation, as well as diffuse and focal cortical abnormalities, alterations of the deep gray matter and involvement of the corpus callosum. Some of the reported changes are associated with seizure and epilepsy, which are observed during HCM and as neurological sequelae [137]. These data, however, cannot be generalized to adult HCM, which varies in clinical course and pathophysiology [118] and for which only a very limited number of MRI studies are available [137]. Published data on MRI findings in adults is principally restricted to a small number of case studies [139-141]. For example, in one such study where four HCM patients were treated, not all patients presented hemorrhages and one patient, who was already in a coma at admission, had suffered acute hemorrhagic infarctions of the brain stem and cerebellum did not survive [141]. However, there are important limitations to MRI and CT scanning and the lack of sensitivity requires significant changes (i.e. hemorrhages, infarct, edema) for detection [142]. In a primate model of CM, for which Japanese macaques (*Macaca fuscata*) were infected with *Plasmodium coatneyi*, positron emission tomography with ^{18}F-fluorodeoxyglucose (FDG-PET) and MRI revealed a reduction of the metabolism in the cerebral cortex, but no significant changes were observed by MRI [143]. It is noteworthy that an MRI study of ECM-resistant mice found increased blood flow and metabolic changes in the brains of infected mice consistent with the observed liver damage, reportedly a feature in human disease [144]. These approaches, while invaluable for clinical diagnoses and treatment, do not inform us on the underlying mechanisms of cerebral malaria pathophysiology. Although some options have become available to study the blood flow alterations associated with HCM, for example orthogonal polarization spectral imaging of the rectal or sublingual mucosa [145-147], computer tomography [148], or magnetic resonance spectroscopy [144], the behavior of individual parasites or immune cells cannot be monitored at high resolution in the brain or in other large internal organs such as the liver or the lung. Postmortem studies provide valuable, but limited information regarding the spatial and temporal progress of parasitological and pathological processes in malaria patients. Small animal models also have limitations in that different host/parasite combinations may exhibit different manifestations of the disease, in some cases somewhat dissimilar from humans. Provided that such results are interpreted cautiously and correlated with knowledge of human disease, animal models are invaluable for study of the biology of the parasite and the pathogenesis of the disease dynamics [149-151].

2.2 Imaging approaches for the live mouse brain

While two-photon microscopy undoubtedly provides advantages in terms of tissue penetration and heat production, confocal microscopy allows data acquisition to a depth of

50 μm in the brain [86, 152] and even in a dense organ such as the liver [3, 4]. Other factors concerning brain IVM enter the equation as well. For example, imaging through a cover-slipped cranial window permits examination of a considerably larger area (~20,000 μm^2) compared to the thinned skull technique (~30 μm^2) [153, 154]. While the thinned skull technique requires two-photon microscopy for penetration of the remaining layer of bone, confocal microscopy readily reaches the superficial cortical microvasculature thorough the intact Dura mater. Preserving the Dura mater is crucial to prevent injury to the cerebral cortex and bleeding from pial vessels, which essentially prevents image acquisition. This approach allows monitoring microvessels in the neocortical layer I of the murine brain [155], i.e. beyond the 10-15 μm thick meninges [86].

2.3 Imaging experimental cerebral malaria

Several approaches have been developed for imaging live mice during ECM, namely whole animal bioluminescence imaging [156, 157], MRI [158, 159], and IVM [86, 160, 161]. Insights gleaned from each of the techniques outlined above will be described here as pertains to ECM.

Parasite sequestration: Infection with *P. berghei* GFP-luciferase$_{SCH}$, a transgenic line that expresses a cytoplasmic GFP-luciferase fusion protein under the schizont-specific promoter *ama1*, revealed CD36-dependent sequestration of parasitized red blood cells within the adipose tissue and the lungs, but surprisingly not in the brains of mice with ECM [128, 157]. On the other hand, bioluminescence imaging of PbA parasites that express luciferase throughout the erythrocytic cycle documented parasite biomass in the brains of mice at the time of ECM, although the signal in the head region was generally small compared to the rest of the body [133, 134, 162, 163]. Further, *ex vivo* imaging revealed random luciferase signal patterns in the brain, suggesting that parasite accumulation is likely not associated with a specific subregion [134, 163]. In the absence of any known adhesion receptors for PbA iRBC other than CD36, together with the lack of PbA iRBC marginalization in the cortical microvasculature [86], factors such as cerebral congestion and hemorrhaging, which likely culminate during the agonal phase of the disease in response to intracranial hypertension, could contribute to the observed accumulation of early-stage iRBC, in particular since prevention of ECM by elimination of CD8+ or CD4+ T cells diminished the luciferase signal in the brain [162, 163]. Interestingly, adherence to CD36 has not yet been conclusively correlated to disease severity in humans (reviewed in [164]). Further, a *P. berghei* gene, schizont membrane associated cytoadherence (*smac*), implicated in CD36-mediated sequestration was shown to be necessary for normal parasite growth indicating a role other than immune evasion for sequestration [165]. *P. berghei Δsmac* were no longer able to sequester *in vivo* and exhibited a reduced growth rate and reduced persistence in the host not solely attributable to RBC removal by the spleen. Indeed, in *in vivo* growth assays, where mixed populations of wt and mutant parasites were transferred weekly to naïve mice, *Δsmac* parasites were undetectable by week 2. In contrast, in splenectomized mice mutant parasites persisted for up to 4 weeks. Restoration of parasite presence in the host to the same levels as wt parasites was only achieved in splenectomized CD36 deficient mice suggesting a role other than avoidance of splenic clearance for CD36 sequestration [165].

Accumulation of platelets and leukocytes: Advances in nano- and micro-particle technology have provided further tools in neuroimaging enabling *in vivo* molecular magnetic resonance imaging (mMRI) of cerebral microvascular endothelial targets such as VCAM-1, E-selectin and markers of activated platelets [166, 167]. Microparticles of iron oxide (MPIO) conjugated to a single chain antibody specific for ligand-induced binding sites on activated platelets glycoprotein IIa/IIIb enable the detection of platelet accumulation in live mice by mMRI [159]. Platelet accumulation was discernible from day 5, with an increase at day 6

and peak at the onset of ECM at day 7. Moreover, platelet accumulation in the cerebral vasculature could be mimicked by intrastriatal injection of TNF-α in uninfected mice [159]. Further development of specific contrasting agents may enable some visualization of cellular interactions in patients if this technology becomes available for safe application in clinical settings.

IVM is currently the only approach that enables the investigation of parasite/host interactions at the cellular level. Quantification of blood flow, cellular adhesion, and leukocyte recruitment can all be achieved with this method [86, 160, 168, 169]. Improvements in reporter fluorescent proteins such as mCherry with increased photostability now provide better tools for this rapidly advancing field [81]. Previous IVM studies have shown that ECM is associated with vasoconstriction and vascular collapse, predominantly of pial arterioles, and leukocyte recruitment mediated by TNF-α [160, 168]. Treatment of mice with nimodipine, a calcium channel blocker used for the treatment of post-subarachnoid hemorrhage (SAH) vasospasm, in conjunction with the antimalarial artemether improved survival of ECM, and in one case led to complete remission without neurological sequelae [160]. Furthermore, a recent IVM study revealed a striking difference in the integrity of the BBB between two lethal *Plasmodium* infections, *P. berghei* ANKA (PbA), a model for ECM, and *P. yoelii* 17XL (PyXL), a model for hyperparasitemia and severe anemia (Figure 3). In this study, young CBA/CaJ mice proved superior for brain imaging based on the anatomical features of their skull and higher tolerance to anesthetics compared to the more traditional ECM model mice (Swiss Webster or C57Bl/6), despite a somewhat higher risk of bleeding during craniotomy due to the higher vascular density in their calvarium [86]. No other approach could have led to the discovery that CBA/CaJ mice with ECM, but not hyperparasitemia, exhibit extensive vascular leakage from postcapillary venules (PCV), but not capillaries or arterioles. Vascular leakage from PCV, the morphological correlate of the neuroimmunological BBB [170], was accompanied by platelet marginalization, extravascular fibrin deposition, and the appearance of endothelial CD14 (Video S3). Blockage of LFA-1 mediated cellular interactions prevented leukocyte adhesion, vascular leakage, neurological signs, and death from ECM.

2.4 Mechanism of BBB opening

Monitoring luciferase-expressing parasites in live mice has demonstrated the requirement for the simultaneous brain accumulation of PbA iRBC and CD8+ effector T cells [133, 134, 157, 162, 163, 171, 172]. Recently, a pro-ECM role was described for IL-12Rβ2, which is predominantly expressed on activated T cells [173]. Using MRI and magnetic resonance angiography (MRA), the authors showed that IL-12 Rβ2 knockout mice did not develop ECM nor showed signed of ECM-associated brain edema or reduced blood flow (due to changes in vascularization). However, ECM onset also requires sufficient parasite-specific antigen to be present [134]. The proposed mechanism of BBB disruption, a hallmark of ECM and HCM has not yet been fully elucidated and evidence is contradictory at times. For example, it has been reported that *P. falciparum* iRBC induce endothelial cell apoptosis *in vitro* by modulating the expression of several genes such as the TNF-α superfamily genes (*Fas*, *Fas* L) and apoptosis-related genes (e.g. *Bad*, *Bax*, *Caspase-3*, *SARP 2*, *IFN-γ*, *iNOS*) leading to morphologically characteristic changes consistent with apoptosis [174]. Further, CD36 activation through trompospondin-1 was shown to induce caspase activation leading to endothelial cell apoptosis [175]. In contrast, in murine models of ECM, resistance to disease was associated with perforin- and granzyme B-mediated cytotoxic effects of CD8+ T cells [134, 135]. There is also evidence of non-apoptotic disruption of BBB tight junction (TJ) proteins by antigen-specific CD8+ T cells in an *in vivo* model of CD8+ T cell-initiated CNS vascular disruption [158]. Moreover, using cultures of human cerebral vasculature cell lines, one study found changes in TJ proteins to be associated with metabolic acidosis and

independent of *P. falciparum* cytoadherence [176], while in another reported opening of intercellular junctions was associated with *P. falciparum* iRBC binding and formation of transmigration-like cups [177].

There is growing evidence from the CNS barrier literature that tight and/or adherens junction protein modification or degradation is sufficient to cause BBB dysregulation including increased permeability and loss of immuno-quiescence (reviewed in [178]). For example, vascular endothelial growth factor (VEGF) has been shown to promote Tyr-phosphorylation of TJ proteins zonula occludens-1 (ZO-1) and occludin either directly through its membrane tyrosine kinase receptor (VEGFR2) or through activation of the cytosolic tyrosine kinase c-src leading to TJ destabilization and increased permeability. It is noteworthy that VEGF has been implicated in the pathology of malaria-associated ALI/ARDS in a murine model (see below) [179]. Indeed, reductions of VEGF levels in sera protected mice from ALI/ARDS. Furthermore, recent evidence using a CD8+ T cell-induced BBB disruption murine model demonstrated that the inhibition of neuropilin-1 (NRP-1), a VEGF co-receptor that enhances VEGFR2 activation, reduced BBB permeability, brain hemorrhages, and mortality [180]. The underlying molecular interactions should be further investigated by IVM to confirm the molecular players and sequence of events that lead to BBB disruption in ECM.

In a recent IVM study, the endothelial barrier-stabilizing mediator fingolimod inhibited vascular leakage and neurological signs and prolonged survival to ECM [86]. Fingolimod (FTY720) is an FDA-approved orally active immunomodulatory drug that has shown efficacy in clinical trials for the treatment of patients with relapsing multiple sclerosis [181]. Fingolimod down-modulates the expression of S1P1 receptors on the T cell surface, which favors the CCR7-mediated retention in lymph nodes of naïve and central memory T cells, but not effector memory T cells [182]. In chronic autoimmune diseases such as experimental autoimmune encephalomyelitis (EAE), a murine model for multiple sclerosis, fingolimod prevents lymphocyte recruitment from secondary lymphatic tissues to the brain [182, 183]. More relevant for acute infections such as ECM, in particular because the drug has to be administered throughout the course of the disease [86, 184], may be its ability to prevent activation of CD8+ effector T cells in the spleen by decreasing migration and function of CD11c+ dendritic cells and by destabilizing dendritic cell/T cell interactions thus preventing immunological synapse formation [185, 186]. In addition to its involvement in T cell activation and targeting to the brain, fingolimod is also thought to have a directly stabilizing effect on endothelial junctions at the BBB [183, 187-189], which is consistent with the observation that granzyme B and perforin deficient mice do not develop ECM, but nevertheless recruit CD8+ T cells to a similar degree as wt mice [135, 190]. Interestingly, the S1P pathway has also been implicated in *P. falciparum* infections [184, 191-194], but whether BBB opening in humans and mice is regulated by similar mechanisms remains to be determined.

2.5 Parasite sequestration and cause of BBB opening

While it is a well-known fact that different parasite/host combinations exhibit pathogenetic differences, in mice as well as in humans, the underlying molecular basis of this phenomenon is unknown. For example, why do certain reticulocyte-tropic *Plasmodium* species such as PbA, Pb K173, and less frequently also *P. berghei* NK65 [86, 195], induce ECM in some susceptible mouse or rat strains, but not in others (reviewed in [136])? Further, do iRBC, in particular *P. vivax* infected reticulocytes, travel through human brain capillaries at reduced velocity, similar to PbA iRBC during ECM [86]? Unless dynamic high resolution imaging studies are performed, a reduction in velocity of ring-iRBC from non-cytoadherent *Plasmodium* species would go unrecognized, for example in autopsy

specimens. However, this phenomenon has been demonstrated clearly in an *in vitro* model; the Russell lab [196] reported that *P. vivax*-infected reticulocytes travel slower through narrow ducts and that reduction in velocity is correlated with parasite maturity. The fact that endothelial adhesion molecules were absent in this *in vitro* system suggests that the decrease in iRBC velocity was due to a decrease in reticulocyte flexibility. Further, *Plasmodium*-induced changes in host cell membrane fluidity are well documented. Based on these and our own data and the reticulocytosis typically associated with the onset of rodent malaria [197], we propose that other *Plasmodium* species, in particular the reticulocyte-tropic *P. vivax and P. ovale*, can also travel slowly through capillaries - without necessarily causing damage to this part of the microvascular tree.

Transient interactions between *P. falciparum* iRBC and the capillary endothelium may very well contribute to the pathogenesis of HCM. Unfortunately, this hypothesis must remain pure speculation unless dynamic studies to distinguish between iRBC traveling at bloodstream velocity and iRBC transiently interacting with the human cerebral microvasculature can be conducted. However, careful examination of human autopsy specimens may reveal that iRBC located in capillaries differ from those present in PCV in terms of parasite maturity. For example, if capillaries were to harbor predominantly ring stages (physically trapped there at the time of death), while PCV were predominantly lined with trophozoite to schizont stages, this might indicate transient iRBC binding to the former and true cytoadhesion to the latter. In this scenario, iRBC “rolling” would be followed by static cytoadherence – as suggested by Silamut and colleagues, whose quantitative analysis of the microvascular sequestration in *P. falciparum*-infected human brains demonstrated spatial clustering by parasite age in different vessels [198]. Importantly, iRBC “rolling”, but not adhesion, would preserve the blood flow in capillaries, which is required to assure the release of new ring stages into the circulation.

IVM enables the differentiation of cortical capillaries (4-8 μm diameter, thin vascular wall, absence of a perivascular space) from PCV (10-60 μm diameter, presence of a perivascular space, influx of blood from joining capillaries) and from arterioles (10-50 μm diameter, no visible perivascular space, efflux of blood into branching capillaries) [86]. Further, a recent study revealed that PCV and arterioles differ in expression of endothelial CD14 and CD31. *In vivo* immunolabeling revealed that CD31 (PECAM-1) is predominantly expressed on the luminal surface of arteriolar endothelia, while CD14 is present on venous endothelia (in addition to monocytes) of PbA-infected ECM mice. Indeed, CD14 was associated with endothelia from PCV, but not those from arterioles or capillaries, from mice infected with PbA, but not mice infected with PyXL or uninfected controls [86]. Furthermore, and in agreement with the role of endothelial CD14 in mediating leukocyte adhesion to cerebral PCV [199-202], we found that CD14-positive PCV exhibit extensive Evans blue leakage, while CD14-negative arterioles do not [86].

In conclusion, brain IVM has proven a powerful tool for study of the pathogenesis of ECM. No other approach could have revealed the central role of the opening of the neuroimmunological BBB in brain edema, coma and death in cerebral malaria.

3. The Dual Role of the Lung in Malaria

The lung contributes crucially to two stages of the *Plasmodium* life cycle. First, the initial generation of hepatocyte-derived erythrocyte-infective merozoites is released into the pulmonary microvasculature, which places the lung at the intersection between the clinically silent liver phase and the symptomatic blood phase of the infection [4]. Second, the lung is subject to a severe manifestation of malaria, ALI/ARDS, which is characterized by

impairment of oxygen exchange due to widespread inflammation of the alveolar microvasculature [203].

3.1 Merosome arrest in the lung

After budding from *Plasmodium* infected hepatocytes, the first generation of merozoites is released into the microvasculature of the liver as merosomes, large bags of hepatocyte membrane containing dozens of parasites [2, 4, 32]. Merosomes are shuttled out of the liver unharmed, by-passing the gauntlet of highly phagocytic Kupffer cells, and travel to the lungs where they are arrested and efficiently cleared from the bloodstream. After a period of most likely several hours, the hepatocyte-derived membrane disintegrates and (all) merozoites are released from the merosome into the pulmonary bloodstream [4].

One possible explanation for the high efficiency with which the lung clears merosomes from the blood [4] is mechanical trapping. Merosomes may be arrested based on their large size within pulmonary arterioles, i.e. before being able to enter the narrow alveolar capillary bed of the lung. This hypothesis is supported by the fact that the average diameter of extrahepatic merosomes (~13-18 μm) clearly exceeds the 1-4 μm functional diameter of alveolar capillaries [4, 204]. However, merozoites that bud from hepatocytes are also much larger than the hepatic sinusoids (~7 μm), but exit the liver nevertheless [4, 205-207]. Mechanical trapping could result if merosomes were to become more rigid prior to entering the lungs. Arguing against this are *ex vivo* lung imaging data showing merosomes easily adapting to the narrow vascular lumen of small pulmonary vessels (Leberl and Frevert, unpublished data) [4], suggesting that merosomes retain the flexibility needed to squeeze through the pulmonary capillary bed if otherwise unrestricted. Alternatively, the merosomal membrane may contain *Plasmodium*-derived adhesion molecules that bind to the microvascular endothelium. This mechanism, even if not selective for the pulmonary endothelium, would explain the high efficiency of merosome clearance from the blood [4], as the lung represents the first capillary bed merosomes encounter after leaving the liver. The exact site of merosome arrest in the alveolar microvasculature is currently under investigation.

Non-malarial ALI/ARDS—Acute lung injury is a uniform response of the lungs to various infectious, inflammatory, or chemical insults. In humans, ALI/ARDS is commonly associated with systemic illness such as sepsis or trauma and less frequently induced by local insults such as pneumonia, aspiration of gastric acid or inhalation of toxic gases [208, 209]. Various animal models have revealed details on the pathogenetic steps leading to ALI/ARDS [210]. Central to the onset is a shift of the normal anti-thrombotic and anti-inflammatory state of the (tolerant) pulmonary endothelia towards an activated pro-thrombotic and pro-inflammatory phenotype with expression of activators of the clotting system and adhesion molecules for platelets and leukocytes [209]. Neutrophils are key effector cells that accumulate in the lung during the pathogenesis of ALI/ARDS [211-213]. Specific receptor ligand interactions as well as the decreased cellular deformability of the infiltrating activated neutrophils mediate their arrest in the narrow pulmonary microvasculature [214, 215]. Further, monocytes are recruited from the bone marrow in response to low-level endotoxemia and marginalize in the pulmonary microvasculature; this predisposes the lungs towards acute injury by secondary septic stimuli [216]. Once attached to the endothelium, macrophages function as a local source of proinflammatory and vasoactive mediators; this eventually causes the breakdown of the blood alveolar barrier (BAB) and flooding of the alveolar space with a proteinaceous edematous fluid. Elimination of inflammatory macrophages or blockage of platelet activation prior to septic challenge attenuates the development of ALI/ARDS [216]. Unlike most animal models of ALI/ARDS, where respiratory failure is typically induced by a single defined stimulus, typically by

intratracheal instillation of noxious materials [217, 218], experimental severe malaria offers the unique opportunity to study these pulmonary complications in a natural multifactorial setting, a situation that resembles closely the redundant stimuli that normally trigger ALI/ARDS in humans [209, 210].

3.2 ALI/ARDS in human severe malaria

Pulmonary complications have long been described primarily for adult patients with malaria [117]. Initially believed to be a severe manifestation restricted to infections with *P. falciparum*, the most fatal of all *Plasmodium* species, case reports during the past 20 years document ALI and ARDS for *P. vivax*, *P. ovale*, and *P. knowlesi* as well [219-227]. Both ALI and ARDS require the presentation of bilateral pulmonary infiltrates on chest radiographs, confirming a pulmonary edema that is neither cardiogenic nor hydrostatic. The resulting impairment of gas exchange is indicated by the ratio of arterial oxygenation to fraction of inspired oxygen (PaO_2/FiO_2), which measures <300 mm Hg for ALI and <200 mm Hg for ARDS compared to 500-300 mm Hg in a normal lung [218, 228-233]. Studies of malaria-associated lung pathology show non-cardiogenic pulmonary edema classified as ALI/ARDS, while the mechanism of interstitial and alveolar flooding with protein-rich fluid is still not entirely clear. Unlike ALI/ARDS induced by sepsis, the infiltration of inflammatory cells into the microvasculature and interstitium of the lung during human malaria appears histopathologically as predominantly mononuclear with a lesser contribution of polymorphnuclear cells [219, 222, 223, 225, 234, 235]. Initially, *P. falciparum* iRBC tether and roll along the microvascular endothelium via interactions with ICAM-1, VCAM-1, PECAM-1, as well as P- and E-selectins, then firmly adhere to endothelial CD36 [117, 221, 236]. The binding of iRBC to the pulmonary microvasculature activates the endothelium and leukocytes, although the relative contribution of the various leukocyte subpopulations remains unclear. Endothelial activation results in the release of cytokines and up-regulation of adhesion molecules, thus perpetuating the inflammatory cell recruitment. This then leads to the accumulation of monocytes, which also release pro-inflammatory cytokines such as TNF-α and IL-1. TNF-α and IL-1, in turn, induce IL-6 and IL-8 as well as endothelial cytoadherence by up-regulating ICAM-1 and VCAM-1, but not CD36 [117, 231, 236]. Although the central role of the pulmonary microvascular injury is now recognized, the relative contribution of individual subsets of inflammatory cells to the disruption of the BAB in humans remains unclear.

3.3 Murine model for malaria-associated ALI/ARDS

Several studies have employed mouse models to study lung pathology prior to death from ECM [237, 238] or in concert with ECM [239-241]. Selective models for murine malaria-associated ALI/ARDS have provided valuable insights into various pathogenetic mechanisms [179, 242, 243] and possible interventions [179, 237, 238, 243, 244]. For example, CD36 is expressed on capillary and post-capillary venule endothelia where it is recognized by *P. berghei* iRBC in the mouse and *P. falciparum* iRBC in humans [245]. The schizont membrane-associated cytoadherence protein (SMAC) of *P. berghei* was identified as a ligand to endothelial CD36 analogous to *P. falciparum* erythrocyte membrane protein 1 (PfEMP1) [165]. CD36 is predominantly expressed in the microvasculature of the lung, adipose tissues, skin, and spleen, but not in the brain [236, 245, 246], and in agreement with its proposed role in *P. berghei* iRBC sequestration in the lung, CD36-deficient mice are protected from malarial ALI [157, 237, 245].

Similar to human and murine CM (see above), Ang-1 also protects against ALI/ARDS by binding to the endothelial receptor Tie2 [217, 247]. Ang-1 counteracts VEGF, a signaling protein involved in the induction of ALI/ARDS [248], while VEGF over-expression closely correlates with decreased levels of Ang-1 [249, 250]. VEGF binding to the endothelial

receptor VEGFR2 reduces VE-cadherin expression in adherens junctions, thus loosening inter-endothelial contacts and increasing vascular permeability, leading to interstitial edema [249, 251]. VEGF over-expression results in the release of various cytokines (TNF-α, IL-1β, IL-6, and IL-8), which cause endothelial adhesion of activated leukocytes leading to vascular permeability in a dose-dependent manner [252, 253]. Carbon monoxide, which reduces the plasma levels of VEGF, has been used as an anti-inflammatory therapy to protect mice from malaria-induced ALI/ARDS [179, 244]. Thus, the cascade of events leading up to the recruitment of inflammatory cells is only partially known and many pathogenetic mechanisms are yet to be discovered.

3.4 Real-time microscopic lung imaging

IVM and *ex vivo* imaging of the intact perfused lung have long been on the forefront of pulmonary research [254-257]. Compared to *ex vivo* imaging, IVM provides normal blood pressure and flow conditions, preserved innervation, an intact immune system, and physiologic ventilation conditions. Various thoracic windows have been constructed for use in dogs [258-260], rabbits [261], and rats [262-265]. To allow microscopic observation of this organ during continued respiratory motion, pulmonary windows have traditionally consisted of a round aluminum or stain-less steel frame, whose exterior upper and lower flanges are implanted into the opening in the chest wall. The frame holds a standard coverslip and is surrounded by a circular suction ring to immobilize the pleural surface of the lung within the viewing area [258, 261-263]. While technically feasible in larger animals, implantation of a thoracic chamber for complete immobilization the lung is more difficult to achieve in mice due to their smaller size and higher respiratory rate. One approach that was exploited extensively for the real-time study of cellular and molecular responses in the mouse lung was to use an *ex vivo* organ model, which allows tight control of inflation and vascular perfusion [266]. *In situ* IVM of the murine lung was only recently accomplished by generating a thoracic window using a flexible transparent polyvinylidene membrane tightly sealed to the rib cage [267]. A trans-diaphragmatic catheter was implanted to remove the intrathoracic air. While this approach brings the re-inflated lung to the polyvinylidene membrane, it does not immobilize the lung under the membrane. Consequently, substantial breathing motion, in addition to artifacts caused by cardiac movements, can be seen in the supplemental online movies, acquired through 10× or 20× objectives with a silicone intensified monochromatic tube camera and recorded on digital videotape [267]. To address this problem, the ventilator was temporarily stopped during the expiratory plateau phase while the lung was allowed to move freely through the respiratory cycle, which permitted digital videotaping of pulmonary microvessels for periods of up to 5 seconds [267]. Another approach is based on open thorax examination of the ventilated mouse lung in a model that relies on low magnification analysis during temporary immobilization of the lung within a suction ring of 2-3 mm diameter [268]. Finally, a novel instrument equipped with a multi-wavelength laser scanner was recently developed that uses needle-sized (1.3 mm diameter) “stick lenses”, which can be inserted deep (1-2 cm) into tissues through a small keyhole incision and allows real-time imaging of most internal organs [269, 270]. Due to the surprisingly high numerical aperture of these stick lenses, this new technology has great potential for future IVM work [271].

3.5 IVM of the *Plasmodium* infected lung

Based on the PbA-infected DBA/2 mouse model for ALI/ARDS [179], we developed a technique for lung IVM to monitor cellular interactions in the pulmonary microvasculature at high-resolution by confocal microscopy. Visualizing the pathogenesis of ALI/ARDS in a live mouse is a difficult task considering the severe respiratory problems presented during the acute phase of the disease. Successful experiments require mice to survive a series of steps including anesthesia, intubation and mechanical ventilation, thoracotomy and

implantation of a pleural window, inoculation of fluorescent markers and long-term imaging, while blood flow and oxygenation are maintained at physiological levels. The model relies on synchronization of respiratory and confocal scan rate, which allows recording of identical phases of the ventilation cycle, for example at the peak of inspiration, thus mimicking complete immobilization of the lung. Restoration of the natural negative intra-thoracic pressure induces close apposition of the pleura during mechanical ventilation further facilitating long-term imaging despite the relatively slow image acquisition rate provided by confocal microscopy (Figure 4, Video S4). This approach, combined with fluorescent parasites, plasma markers, and probes for specific leukocyte subpopulations and platelets, revealed that ALI/ARDS in the PbA-infected DBA/2 mouse model manifests as acute microvascular injury and interstitial pneumonia with a mononuclear infiltrate composed predominantly of blood-derived monocytes/macrophages, dendritic cells, and CD8+ T cells (Leberl and Frevert, manuscript in preparation). This murine lung IVM model sets the stage for further studies on the mechanism of the BAB dysfunction and hemodynamic changes associated with ALI/ARDS or other forms of severe malaria. Beyond malaria, lung IVM offers the opportunity to monitor immune cell interactions and microvascular alterations involved in the pathogenesis of other apicomplexan parasites such as *Toxoplasma gondii*, nematodes or flukes with a developmental or larval migration phase in the lung, for example *Paragonimus*, *Schistosoma*, or *Strongyloides*, and various forms of bacterial, viral and fungal pneumonia.

Outlook

Intravital microscopy (IVM) has grown steadily since its first publication in 1839 [272], with currently over 200 papers being published annually [273]. Although restricted to analysis of superficial tissue layers, IVM, whether by bright field/digital, confocal, two-photon or spinning disk microscopy, is currently the only way to study the dynamics of individual cell interactions *in vivo*. Due to scattering of emitted signal, deep layers of skin or internal organs may never be accessible to high-resolution microscopic imaging. Whole animal imaging provides information on overall parasite mass, but not parasite number [274]. Late-stage blood parasites express the greatest luciferase signal due to their large size so that a given signal intensity may reflect a large number of early-stage iRBC (high parasitemia) or a much smaller number of late-stage parasites, unless schizont-specific fluorescent protein constructs are used [275]. Further, the influence on the luminescence signal intensity of factors such as tissue density and parasite depth within the body or organ is difficult to ascertain. Detection of low intensity signal may require organ removal and *ex vivo* analysis at increased detector sensitivity. Further, whole animal imaging lacks the resolution to distinguish truly arrested from slowly moving iRBC so that vascular congestion may simulate parasite accumulation. Thus, whole body imaging, similar to qPCR, is semi-quantitative and cannot reveal parasite sequestration or immune cell recruitment in the strict sense. Flow cytometry does provide quantitative and molecular information, but requires that cells be removed from their natural microenvironment. Histological tissue sections are subject to fixation and therefore only provide a snapshot in time - and not necessarily an accurate one, because manipulations of the animal prior to organ harvest may influence the apparent histopathology to a larger extent than the disease process itself. For example, the circumstances surrounding the death of the experimental animal, whether due to the disease or by sacrifice, the type of anesthesia, alteration of the vascular content by exsanguination or vascular perfusion, as well as the method of organ harvesting all influence the apparent histopathological outcome. In conclusion, no one methodology can provide the ultimate answer. Therefore, by interpreting different approaches such as IVM and whole mouse imaging, immunohistochemistry and histopathology, cytokine measurements and flow cytometric quantification of cell

populations and their state of activation in conjunction, we will eventually be able to decipher the immunobiology of *Plasmodium* and the pathogenesis of malaria.

Supplementary Material

Refer to Web version on PubMed Central for supplementary material.

Acknowledgments

The authors declare no conflict of interest.

References

1. WHO. World Malaria Report: 2011, in WHO Global Malaria Programme. World Health Organization; Geneva, Switzerland: 2011.
2. Sturm, A.; Amino, R.; van de Sand, C.; Regen, T.; Retzlaff, S.; Rennenberg, A.; Krueger, A.; Pollok, JM.; Menard, R.; Heussler, VT. Science. Vol. 313. New York, N.Y.: 2006. Manipulation of host hepatocytes by the malaria parasite for delivery into liver sinusoids; p. 1287-90.
3. Frevert U, Engelmann S, Zougbédé S, Stange J, Ng B, Matuschewski K, Liebes L, Yee H. Intravital observation of *Plasmodium berghei* sporozoite infection of the liver. PLoS Biol. 2005; 3(6):e192. [PubMed: 15901208]
4. Baer K, Klotz C, Kappe SHIK, Schnieder T, Frevert U. Release of hepatic *Plasmodium yoelii* merozoites into the pulmonary microvasculature. PLoS Pathog. 2007; 3(11):e171. [PubMed: 17997605]
5. MacSween, RNM.; Desmet, VJ.; Roskams, T.; Scothorne, RJ. Developmental anatomy and normal structure, in Pathology of the Liver. MacSween, RNM.; Burt, AD.; Portmann, BC.; Ishak, KG.; Scheuer, PJ.; Anthony, PP., editors. Churchill Livingstone; New York: 2002. p. 1-66.
6. Floch, MH. Netter's Gastroenerology. 2. Philadelphia, PA: Saunders, Elsevier; 2010.
7. Racanelli V, Rehermann B. The liver as an immunological organ. Hepatology. 2006; 43(2 Suppl 1):S54–62. [PubMed: 16447271]
8. Crispe IN. The liver as a lymphoid organ. Annu Rev Immunol. 2009; 27:147–63. [PubMed: 19302037]
9. Knolle PA, Gerken G. Local control of the immune response in the liver. Immunol Rev. 2000; 174:21–34. [PubMed: 10807504]
10. Babbey CM, Ryan JC, Gill EM, Ghabril MS, Burch CR, Paulman A, Dunn KW. Quantitative intravital microscpy of hepatic transport. IntraVital. 2012; 1(1):1–10.
11. McDonald B, McAvoy EF, Lam F, Gill V, de la Motte C, Savani RC, Kubes P. Interaction of CD44 and hyaluronan is the dominant mechanism for neutrophil sequestration in inflamed liver sinusoids. J Exp Med. 2008; 205(4):915–27. [PubMed: 18362172]
12. Crispe IN. Liver antigen-presenting cells. J Hepatol. 2011; 54(2):357–65. [PubMed: 21084131]
13. McCuskey RS, Urbaschek R, McCuskey PA, Urbaschek B. In vivo microscopic observations of the responses of Kupffer cells and the hepatic microcirculation to *Mycobacterium bovis* BCG alone and in combination with endotoxin. Infect Immun. 1983; 42:362–367. [PubMed: 6352499]
14. Li C, McCuskey P, Kan Z, Yang DJ, Wright KC, Wallace S. In vivo and electron microscopic studies of rat liver after intravenous injection of polyamino acid microspheres. J Biomed Mater Res. 1994; 28(8):881–90. [PubMed: 7527046]
15. Eguchi H, McCuskey PA, McCuskey RS. Kupffer cell activity and hepatic microvascular events after acute ethanol ingestion in mice. Hepatology. 1991; 13(4):751–7. [PubMed: 2010170]
16. McCuskey RS, McCuskey PA, Eguchi H, Crichton EG, Urbaschek R, Urbaschek B. In vivo microscopy of the liver following acute administration of ethanol. Prog Clin Biol Res. 1990; 325:341–50. [PubMed: 2300616]
17. Ivancev K, Lunderquist A, McCuskey R, McCuskey P, Wretlind A. Effect of intravenously injected iodinated lipid emulsion on the liver. An experimental study correlating computed

tomography findings with in vivo microscopy and electron microscopy findings. Acta Radiol. 1989; 30(3):291–8. [PubMed: 2544217]

18. Post S, Gonzalez AP, Palma P, Rentsch M, Stiehl A, Menger MD. Assessment of hepatic phagocytic activity by in vivo microscopy after liver transplantation in the rat. Hepatology. 1992; 16(3):803–9. [PubMed: 1505924]
19. Farrell GC, Teoh NC, McCuskey RS. Hepatic microcirculation in fatty liver disease. Anat Rec (Hoboken). 2008; 291(6):684–92. [PubMed: 18484615]
20. Cara DC, Kubes P. Intravital microscopy as a tool for studying recruitment and chemotaxis. Methods Mol Biol. 2004; 239:123–32. [PubMed: 14573914]
21. McDonald B, Pittman K, Menezes GB, Hirota SA, Slaba I, Waterhouse CC, Beck PL, Muruve DA, Kubes P. Intravascular danger signals guide neutrophils to sites of sterile inflammation. Science. 2010; 330(6002):362–6. [PubMed: 20947763]
22. McDonald B, Kubes P. Neutrophils and intravascular immunity in the liver during infection and sterile inflammation. Toxicol Pathol. 2012; 40(2):157–65. [PubMed: 22105645]
23. Phillipson M, Kubes P. The neutrophil in vascular inflammation. Nat Med. 2011; 17(11):1381–90. [PubMed: 22064428]
24. Menezes GB, Mansur DS, McDonald B, Kubes P, Teixeira MM. Sensing sterile injury: opportunities for pharmacological control. Pharmacol Ther. 2011; 132(2):204–14. [PubMed: 21763344]
25. Wong CH, Heit B, Kubes P. Molecular regulators of leucocyte chemotaxis during inflammation. Cardiovasc Res. 2010; 86(2):183–91. [PubMed: 20124403]
26. Geissmann F, Cameron TO, Sidobre S, Manlongat N, Kronenberg M, Briskin MJ, Dustin ML, Littman DR. Intravascular immune surveillance by CXCR6+ NKT cells patrolling liver sinusoids. PLoS Biol. 2005; 3(4):e113. [PubMed: 15799695]
27. Egen JG, Rothfuchs AG, Feng CG, Horwitz MA, Sher A, Germain RN. Intravital imaging reveals limited antigen presentation and T cell effector function in mycobacterial granulomas. Immunity. 2011; 34(5):807–19. [PubMed: 21596592]
28. Egen JG, Rothfuchs AG, Feng CG, Winter N, Sher A, Germain RN. Macrophage and T cell dynamics during the development and disintegration of mycobacterial granulomas. Immunity. 2008; 28(2):271–84. [PubMed: 18261937]
29. Pittet MJ, Weissleder R. Intravital imaging. Cell. 2011; 147(5):983–91. [PubMed: 22118457]
30. Ritsma L, Ponsionen B, van Rheenen J. Intravital imaging of cell signaling in mice. IntraVital. 2012; 1(1):2–10.
31. Meis JFGM, Verhave JP. Exoerythrocytic development of malaria parasites. Adv Parasitol. 1988; 27:1–61. [PubMed: 3289327]
32. Tarun AS, Baer K, Dumpit RF, Gray S, Lejarcegui N, Frevert U, Kappe S. Quantitative isolation and *in vivo* imaging of malaria parasite liver stages. Int J Parasitol. 2006; 36(12):1283–1293. [PubMed: 16890231]
33. van de Sand C, Horstmann S, Schmidt A, Sturm A, Bolte S, Krueger A, Lutgehetmann M, Pollok JM, Libert C, Heussler VT. The liver stage of *Plasmodium berghei* inhibits host cell apoptosis. Mol Microbiol. 2005; 58(3):731–42. [PubMed: 16238623]
34. Rankin KE, Graewe S, Heussler VT, Stanway RR. Imaging liver-stage malaria parasites. Cell Microbiol. 2010; 12(5):569–79. [PubMed: 20180802]
35. Frevert U, Sinnis P, Cerami C, Shreffler W, Takacs B, Nussenzweig V. Malaria circumsporozoite protein binds to heparan sulfate proteoglycans associated with the surface membrane of hepatocytes. J Exp Med. 1993; 177:1287–1298. [PubMed: 8478608]
36. Pradel G, Garapaty S, Frevert U. Proteoglycans mediate malaria sporozoite targeting to the liver. Mol Microbiol. 2002; 45(3):637–651. [PubMed: 12139612]
37. Cerami C, Frevert U, Sinnis P, Takacs B, Clavijo P, Santos MJ, Nussenzweig V. The basolateral domain of the hepatocyte plasma membrane bears receptors for the circumsporozoite protein of *Plasmodium falciparum* sporozoites. Cell. 1992; 70:1021–1033. [PubMed: 1326407]
38. Cerami C, Frevert U, Sinnis P, Takacs B, Nussenzweig V. Rapid clearance of malaria circumsporozoite protein (CS) by hepatocytes. J Exp Med. 1994; 179:695–701. [PubMed: 8294876]

39. Pradel G, Frevert U. *Plasmodium* sporozoites actively enter and pass through Kupffer cells prior to hepatocyte invasion. Hepatology. 2001; 33:1154–1165. [PubMed: 11343244]
40. Pradel G, Garapaty S, Frevert U. Kupffer and stellate cell proteoglycans mediate malaria sporozoite targeting to the liver. Comp Hepatol. 2004; 3(1):S47. [PubMed: 14960199]
41. Baer K, Roosevelt M, Van Rooijen N, Clarkson AB Jr, Schnieder T, Frevert U. Kupffer cells are obligatory for *Plasmodium* sporozoite infection of the liver. Cell Microbiol. 2007; 9:397–412. [PubMed: 16953803]
42. Frevert U, Usynin I, Baer K, Klotz C. Nomadic or sessile: can Kupffer cells function as portals for malaria sporozoites to the liver? Cell Microbiol. 2006; 8:1537–1546. [PubMed: 16911567]
43. Frevert U, Usynin I, Baer K, Klotz C. Plasmodium sporozoite passage across the sinusoidal cell layer. Subcell Biochem. 2008; 47:182–97. [PubMed: 18512352]
44. Mota MM, Pradel G, Vanderberg JP, Hafalla JCR, Frevert U, Nussenzweig RS, Nussenzweig V, Rodriguez A. Migration of *Plasmodium* sporozoites through cells before infection. Science. 2001; 291:141–144. [PubMed: 11141568]
45. Meis JF, Verhave JP, Jap PH, Meuwissen JH. An ultrastructural study on the role of Kupffer cells in the process of infection by *Plasmodium berghei* sporozoites in rats. Parasitology. 1983; 86:231–242. [PubMed: 6343960]
46. Meis JFGM, Verhave JP, Brouwer A, Meuwissen JHET. Electron microscopic studies on the interaction of rat Kupffer cells and *Plasmodium berghei* sporozoites. Z Parasitenkd. 1985; 71:473–483. [PubMed: 3895767]
47. Tavares J, Formaglio P, Thiberge S, Mordelet E, Van Rooijen N, Medvinsky A, Menard R, Amino R. Role of host cell traversal by the malaria sporozoite during liver infection. J Exp Med. 2013; 210(5):905–15. [PubMed: 23610126]
48. Frevert U, Späth G, Gregg Y. Exoerythrocytic development of *Plasmodium gallinaceum* in the White Leghorn chicken. Int J Parasitol. 2008; 38(6):655–72. [PubMed: 18005972]
49. Huff CG. Recent experimental research on avian malaria. Adv Parasitol. 1968; 6:293–311. [PubMed: 4389251]
50. Usynin I, Klotz C, Frevert U. Malaria circumsporozoite protein inhibits the respiratory burst in Kupffer cells. Cell Microbiol. 2007; 9(11):2610–28. [PubMed: 17573905]
51. Klotz C, Frevert U. Plasmodium yoelii sporozoites modulate cytokine profile and induce apoptosis in murine Kupffer cells. Int J Parasitol. 2008; 38(14):1639–50. [PubMed: 18656478]
52. Krzych, U.; Guebre-Xabier, M.; Schwenk, R. Malaria and the liver: tolerance and immunity to attenuated Plasmodium sporozoites, in T Lymphocytes in the Liver: Immunobiology, Pathology, and Host Defence. Crispe, IN., editor. John Wiley & Sons, Inc.; New York: 1999. p. 163-195.
53. Klotz C, Frevert U. *Plasmodium* sporozoites modulate cytokine secretion profile and induce apoptosis in murine Kupffer cells. Int J Parasitol. 2008; 38(14):1639–50. [PubMed: 18656478]
54. Usynin I, Klotz C, Frevert U. Malaria circumsporozoite protein inhibits the respiratory burst in Kupffer cells. Cell Microbiol. 2007; 9:2610–2628. [PubMed: 17573905]
55. Ishino T, Yano K, Chinzei Y, Yuda M. Cell-passage activity is required for the malarial parasite to cross the liver sinusoidal cell layer. PLoS Biol. 2004; 2(1):E4. [PubMed: 14737184]
56. Vanderberg JP, Chew S, Stewart MJ. *Plasmodium* sporozoite interactions with macrophages in vitro: a videomicroscopic analysis. J Protozool. 1990; 37:528–536. [PubMed: 2086782]
57. Frevert U, Usynin I, Baer K, Klotz C. Nomadic or sessile: can Kupffer cells function as portals for malaria sporozoites to the liver? Cell Microbiol. 2006; 8(10):1537–46. [PubMed: 16911567]
58. Wiktor-Jedrzejczak W, Gordon S. Cytokine regulation of the macrophage (Mθ) system studied using the colony stimulating factor-1-deficient op/op mouse. Physiol Rev. 1996; 76:927–947. [PubMed: 8874489]
59. Kennedy M, Fishbaugher ME, Vaughan AM, Patrapuvich R, Boonhok R, Yimamnuaychok N, Rezakhani N, Metzger P, Ponpuak M, Sattabongkot J, Kappe SH, Hume JC, Lindner SE. A rapid and scalable density gradient purification method for Plasmodium sporozoites. Malar J. 2012; 11:421. [PubMed: 23244590]
60. Jayabalasingham B, Bano N, Coppens I. Metamorphosis of the malaria parasite in the liver is associated with organelle clearance. Cell Res. 2010; 20(9):1043–59. [PubMed: 20567259]

61. Silvie O, Charrin S, Billard M, Franetich JF, Clark KL, van Gemert GJ, Sauerwein RW, Dautry F, Boucheix C, Mazier D, Rubinstein E. Cholesterol contributes to the organization of tetraspanin-enriched microdomains and to CD81-dependent infection by malaria sporozoites. J Cell Sci. 2006; 119(Pt 10):1992–2002. [PubMed: 16687736]
62. Bano N, Romano JD, Jayabalasingham B, Coppens I. Cellular interactions of *Plasmodium* liver stage with its host mammalian cell. Int J Parasitol. 2007; 37(12):1329–41. [PubMed: 17537443]
63. Labaied M, Jayabalasingham B, Bano N, Cha SJ, Sandoval J, Guan G, Coppens I. *Plasmodium* salvages cholesterol internalized by LDL and synthesized de novo in the liver. Cell Microbiol. 2011; 13(4):569–86. [PubMed: 21105984]
64. Deschermeier C, Hecht LS, Bach F, Rutzel K, Stanway RR, Nagel A, Seeber F, Heussler VT. Mitochondrial lipoic acid scavenging is essential for *Plasmodium berghei* liver stage development. Cell Microbiol. 2012; 14(3):416–30. [PubMed: 22128915]
65. Graewe S, Rankin KE, Lehmann C, Deschermeier C, Hecht L, Froehlke U, Stanway RR, Heussler V. Hostile takeover by *Plasmodium*: reorganization of parasite and host cell membranes during liver stage egress. PLoS Pathog. 2011; 7(9):e1002224. [PubMed: 21909271]
66. Luder CG, Stanway RR, Chaussepied M, Langsley G, Heussler VT. Intracellular survival of apicomplexan parasites and host cell modification. Int J Parasitol. 2009; 39(2):163–73. [PubMed: 19000910]
67. Rennenberg A, Lehmann C, Heitmann A, Witt T, Hansen G, Nagarajan K, Deschermeier C, Turk V, Hilgenfeld R, Heussler VT. Exoerythrocytic *Plasmodium* parasites secrete a cysteine protease inhibitor involved in sporozoite invasion and capable of blocking cell death of host hepatocytes. PLoS Pathog. 2010; 6(3):e1000825. [PubMed: 20361051]
68. Sturm A, Graewe S, Franke-Fayard B, Retzlaff S, Bolte S, Roppenser B, Aepfelbacher M, Janse C, Heussler V. Alteration of the parasite plasma membrane and the parasitophorous vacuole membrane during exo-erythrocytic development of malaria parasites. Protist. 2009; 160(1):51–63. [PubMed: 19026596]
69. Terzakis JA, Vanderberg JP, Foley D, Shustak S. Exoerythrocytic merozoites of *Plasmodium berghei* in rat hepatic Kupffer cells. J Protozool. 1979; 26:385–389. [PubMed: 395294]
70. Uhlmann S, Uhlmann D, Spiegel HU. Evaluation of hepatic microcirculation by in vivo microscopy. J Invest Surg. 1999; 12(4):179–93. [PubMed: 10501077]
71. Clemens MG, Zhang JX. Regulation of sinusoidal perfusion: in vivo methodology and control by endothelins. Semin Liver Dis. 1999; 19(4):383–96. [PubMed: 10643624]
72. Pries AR, Gaehtgens P. Digital video image-shearing device for continuous microvessel diameter measurement. Microvasc Res. 1987; 34(2):260–7. [PubMed: 3670118]
73. Ley K, Pries AR, Gaehtgens P. A versatile intravital microscope design. Int J Microcirc Clin Exp. 1987; 6(2):161–7. [PubMed: 3596913]
74. Graf R, Rietdorf J, Zimmermann T. Live cell spinning disk microscopy. Adv Biochem Eng Biotechnol. 2005; 95:57–75. [PubMed: 16080265]
75. Velazquez P, Cameron TO, Kinjo Y, Nagarajan N, Kronenberg M, Dustin ML. Cutting edge: activation by innate cytokines or microbial antigens can cause arrest of natural killer T cell patrolling of liver sinusoids. J Immunol. 2008; 180(4):2024–8. [PubMed: 18250405]
76. Cabrera M, Frevert U. Novel *in vivo* imaging techniques for the liver microvasculature. IntraVital. 2012; 1(2):107–114.
77. Khan ZM, Vanderberg JP. Role of host cellular response in differential susceptibility of nonimmunized BALB/C mice to *Plasmodium berghei* and *Plasmodium yoelii* sporozoites. Infect Immun. 1991; 59:2529–2534. [PubMed: 1855974]
78. Franke-Fayard B, Trueman H, Ramesar J, Mendoza J, van der Keur M, van der Linden R, Sinden RE, Waters AP, Janse CJ. A *Plasmodium berghei* reference line that constitutively expresses GFP at a high level throughout the complete life cycle. Mol Biochem Parasitol. 2004; 137(1):23–33. [PubMed: 15279948]
79. Helm S, Lehmann C, Nagel A, Stanway RR, Horstmann S, Llinas M, Heussler VT. Identification and characterization of a liver stage-specific promoter region of the malaria parasite *Plasmodium*. PLoS One. 2010; 5(10):e13653. [PubMed: 21048918]

80. Kooij TW, Rauch MM, Matuschewski K. Expansion of experimental genetics approaches for *Plasmodium berghei* with versatile transfection vectors. Mol Biochem Parasitol. 2012; 185(1):19–26. [PubMed: 22705315]
81. Graewe S, Retzlaff S, Struck N, Janse CJ, Heussler VT. Going live: a comparative analysis of the suitability of the RFP derivatives RedStar, mCherry and tdTomato for intravital and in vitro live imaging of *Plasmodium* parasites. Biotechnol J. 2009; 4(6):895–902. [PubMed: 19492329]
82. Ploemen I, Behet M, Nganou-Makamdop K, van Gemert GJ, Bijker E, Hermsen C, Sauerwein R. Evaluation of immunity against malaria using luciferase-expressing *Plasmodium berghei* parasites. Malar J. 2011; 10:350. [PubMed: 22152047]
83. Ploemen IHJ, Prudencio M, Douradinha BG, Ramesar J, Fonager J, van Gemert GJ, Luty AJF, Hermsen CC, Sauerwein RW, Baptista FG, Mota MM, Waters AP, Que I, Lowik CWGM, Khan SM, Janse CJ, Franke-Fayard BMD. Visualisation and quantitative analysis of the rodent malaria liver stage by real time imaging. PLoS ONE. 2009; 4(11):e7881. [PubMed: 19924309]
84. Cabrera M, Pewe LL, Harty JT, Frevert U. *In vivo* CD8+ T cell dynamics in the liver of *Plasmodium yoelii* immunized and infected mice. PLoS One. 2013 in press.
85. Jacobs-Lorena VY, Mikolajczak SA, Labaied M, Vaughan AM, Kappe SH. A dispensable *Plasmodium* locus for stable transgene expression. Mol Biochem Parasitol. 2010; 171(1):40–4. [PubMed: 20045029]
86. Nacer A, Movila A, Baer K, Mikolajczak SA, Kappe SH, Frevert U. Neuroimmunological blood brain barrier opening in experimental cerebral malaria. PLoS Pathog. 2012; 8(10):e1002982. [PubMed: 23133375]
87. Menezes GB, Lee WY, Zhou H, Waterhouse CC, Cara DC, Kubes P. Selective down-regulation of neutrophil Mac-1 in endotoxemic hepatic microcirculation via IL-10. J Immunol. 2009; 183(11): 7557–68. [PubMed: 19917697]
88. Nardin E. The past decade in malaria synthetic peptide vaccine clinical trials. Hum Vaccin. 2010; 6(1):27–38. [PubMed: 20173408]
89. Khan SM, Janse CJ, Kappe SH, Mikolajczak SA. Genetic engineering of attenuated malaria parasites for vaccination. Curr Opin Biotechnol. 2012; 23:1–9. [PubMed: 22244690]
90. Sauerwein RW, Bijker EM, Richie TL. Empowering malaria vaccination by drug administration. Curr Opin Immunol. 2010; 22(3):367–73. [PubMed: 20434895]
91. Hoffman SL, Billingsley PF, James E, Richman A, Loyevsky M, Li T, Chakravarty S, Gunasekera A, Chattopadhyay R, Li M, Stafford R, Ahumada A, Epstein JE, Sedegah M, Reyes S, Richie TL, Lyke KE, Edelman R, Laurens MB, Plowe CV, Sim BK. Development of a metabolically active, non-replicating sporozoite vaccine to prevent *Plasmodium falciparum* malaria. Hum Vaccin. 2010; 6(1):97–106. [PubMed: 19946222]
92. Nussenzweig RS, Vanderberg J, Most H, Orton C. Protective immunity produced by the injection of x-irradiated sporozoites of *Plasmodium berghei*. Nature. 1967; 216(5111):160–2. [PubMed: 6057225]
93. Belnoue E, Costa FT, Frankenberg T, Vigario AM, Voza T, Leroy N, Rodrigues MM, Landau I, Snounou G, Renia L. Protective T cell immunity against malaria liver stage after vaccination with live sporozoites under chloroquine treatment. J Immunol. 2004; 172(4):2487–95. [PubMed: 14764721]
94. Renia L, Gruner AC, Mauduit M, Snounou G. Vaccination using normal live sporozoites under drug treatment. Methods Mol Biol. 2013; 923:567–76. [PubMed: 22990805]
95. Purcell LA, Wong KA, Yanow SK, Lee M, Spithill TW, Rodriguez A. Chemically attenuated *Plasmodium* sporozoites induce specific immune responses, sterile immunity and cross-protection against heterologous challenge. Vaccine. 2008; 26(38):4880–4. [PubMed: 18672017]
96. Douradinha B, van Dijk MR, Ataide R, van Gemert GJ, Thompson J, Franetich JF, Mazier D, Luty AJ, Sauerwein R, Janse CJ, Waters AP, Mota MM. Genetically attenuated P36p-deficient *Plasmodium berghei* sporozoites confer long-lasting and partial cross-species protection. Int J Parasitol. 2007; 37(13):1511–9. [PubMed: 17604034]
97. van Dijk MR, Douradinha B, Franke-Fayard B, Heussler V, van Dooren MW, van Schaijk B, van Gemert GJ, Sauerwein RW, Mota MM, Waters AP, Janse CJ. Genetically attenuated, P36p-

deficient malarial sporozoites induce protective immunity and apoptosis of infected liver cells. Proc Natl Acad Sci U S A. 2005; 102(34):12194–12199. [PubMed: 16103357]

98. Richie TL, Haberberger RL. RTS,S/AS01 malaria vaccine in African children. N Engl J Med. 2012; 366(8):765. [PubMed: 22356335]
99. Roestenberg M, McCall M, Hopman J, Wiersma J, Luty AJF, van Gemert GJ, van de Vegte-Bolmer M, van Schaijk B, Teelen K, Arens T, Spaarman L, de Mast Q, Roeffen W, Snounou G, Renia L, van der Ven A, Hermsen CC, Sauerwein R. Protection against a malaria challenge by sporozoite inoculation. New Engl J Med. 2009; 361(5):468–77. [PubMed: 19641203]
100. Butler NS, Schmidt NW, Vaughan AM, Aly AS, Kappe SH, Harty JT. Superior antimalarial immunity after vaccination with late liver stage-arresting genetically attenuated parasites. Cell Host Microbe. 2011; 9(6):451–62. [PubMed: 21669394]
101. Tsuji M. A retrospective evaluation of the role of T cells in the development of malaria vaccine. Exp Parasitol. 2010; 126(3):421–5. [PubMed: 19944099]
102. Overstreet MG, Cockburn IA, Chen YC, Zavala F. Protective CD8 T cells against *Plasmodium* liver stages: immunobiology of an 'unnatural' immune response. Immunol Rev. 2008; 225:272–83. [PubMed: 18837788]
103. Doolan DL, Martinez-Alier N. Immune response to pre-erythrocytic stages of malaria parasites. Curr Mol Med. 2006; 6(2):169–85. [PubMed: 16515509]
104. Krzych U, Schwenk J. The dissection of CD8 T cells during liver-stage infection. Curr Top Microbiol Immunol. 2005; 297:1–24. [PubMed: 16265901]
105. Krzych U, Dalai S, Zarling S, Pichugin A. Memory CD8 T cells specific for plasmodia liver-stage antigens maintain protracted protection against malaria. Front Immunol. 2012; 3:370. [PubMed: 23233854]
106. Nganou-Makamdop K, Ploemen I, Behet M, GJ VANG, Hermsen C, Roestenberg M, Sauerwein RW. Reduced Plasmodium berghei sporozoite liver load associates with low protective efficacy after intradermal immunization. Parasite Immunol. 2012; 34(12):562–9. [PubMed: 23171040]
107. Zarling S, Berenzon D, Dalai S, Liepinsh D, Steers N, Krzych U. The Survival of Memory CD8 T Cells That Is Mediated by IL-15 Correlates with Sustained Protection Against Malaria. J Immunol. 2013; 190(10):5128–41. [PubMed: 23589611]
108. Bongfen SE, Torgler R, Romero JF, Renia L, Corradin G. *Plasmodium berghei*-infected primary hepatocytes process and present the circumsporozoite protein to specific CD8+ T cells *in vitro*. J Immunol. 2007; 178(11):7054–63. [PubMed: 17513754]
109. Rénia L, Marussig MS, Grillot D, Pied S, Corradin G, Miltgen F, Guidice Gd, Mazier D. *In vitro* activity of CD4+ and CD 8+ T lymphocytes from mice immunized with a synthetic malaria peptide. Proc Natl Acad Sci USA. 1991; 88:7963–7967. [PubMed: 1680235]
110. Trimnell A, Takagi A, Gupta M, Richie TL, Kappe SH, Wang R. Genetically attenuated parasite vaccines induce contact-dependent CD8+ T cell killing of *Plasmodium yoelii* liver stage-infected hepatocytes. J Immunol. 2009; 183(9):5870–8. [PubMed: 19812194]
111. Cockburn IA, Amino R, Kelemen RK, Kuo SC, Tse SW, Radtke A, Mac-Daniel L, Ganusov VV, Zavala F, Menard R. In vivo imaging of CD8+ T cell-mediated elimination of malaria liver stages. Proc Natl Acad Sci U S A. 2013
112. Friedl P, Weigelin B. Interstitial leukocyte migration and immune function. Nat Immunol. 2008; 9(9):960–9. [PubMed: 18711433]
113. Schmidt NW, Butler NS, Badovinac VP, Harty JT. Extreme CD8 T cell requirements for anti-malarial liver-stage immunity following immunization with radiation attenuated sporozoites. PLoS Pathog. 2010; 6(7):e1000998. [PubMed: 20657824]
114. Frevert U, Nacer A. Immunobiology of *Plasmodium* in liver and brain. Parasite Immunol. 2013 Apr 30. Epub ahead of print. 10.1111/pim.12039
115. Meister S, Plouffe DM, Kuhen KL, Bonamy GM, Wu T, Barnes SW, Bopp SE, Borboa R, Bright AT, Che J, Cohen S, Dharia NV, Gagaring K, Gettayacamin M, Gordon P, Groessl T, Kato N, Lee MC, McNamara CW, Fidock DA, Nagle A, Nam TG, Richmond W, Roland J, Rottmann M, Zhou B, Froissard P, Glynne RJ, Mazier D, Sattabongkot J, Schultz PG, Tuntland T, Walker JR, Zhou Y, Chatterjee A, Diagana TT, Winzeler EA. Imaging of *Plasmodium* liver stages to drive

next-generation antimalarial drug discovery. Science. 2011; 334(6061):1372–7. [PubMed: 22096101]

116. Schofield L, Grau GE. Immunological processes in malaria pathogenesis. Nat Rev Immunol. 2005; 5(9):722–35. [PubMed: 16138104]
117. Rogerson SJ, Grau GE, Hunt NH. The microcirculation in severe malaria. Microcirculation. 2004; 11(7):559–76. [PubMed: 15513866]
118. Haldar K, Murphy SC, Milner DA, Taylor TE. Malaria: mechanisms of erythrocytic infection and pathological correlates of severe disease. Annu Rev Pathol. 2007; 2:217–49. [PubMed: 18039099]
119. Newton CR, Taylor TE, Whitten RO. Pathophysiology of fatal falciparum malaria in African children. Am J Trop Med Hyg. 1998; 58(5):673–83. [PubMed: 9598460]
120. Grau GE, Mackenzie CD, Carr RA, Redard M, Pizzolato G, Allasia C, Cataldo C, Taylor TE, Molyneux ME. Platelet accumulation in brain microvessels in fatal pediatric cerebral malaria. J Infect Dis. 2003; 187(3):461–6. [PubMed: 12552430]
121. Brown H, Rogerson S, Taylor T, Tembo M, Mwenechanya J, Molyneux M, Turner G. Blood-brain barrier function in cerebral malaria in Malawian children. Am J Trop Med Hyg. 2001; 64(3-4):207–13. [PubMed: 11442219]
122. Brown H, Turner G, Rogerson S, Tembo M, Mwenechanya J, Molyneux M, Taylor T. Cytokine expression in the brain in human cerebral malaria. J Infect Dis. 1999; 180(5):1742–6. [PubMed: 10515846]
123. Beeson JG, Brown GV. Pathogenesis of *Plasmodium falciparum* malaria: the roles of parasite adhesion and antigenic variation. Cell Mol Life Sci. 2002; 59(2):258–71. [PubMed: 11915943]
124. Chakravorty SJ, Craig A. The role of ICAM-1 in *Plasmodium falciparum* cytoadherence. Eur J Cell Biol. 2005; 84(1):15–27. [PubMed: 15724813]
125. Suwanarusk R, Cooke BM, Dondorp AM, Silamut K, Sattabongkot J, White NJ, Udomsangpetch R. The deformability of red blood cells parasitized by *Plasmodium falciparum* and *P. vivax*. J Infect Dis. 2004; 189(2):190–4. [PubMed: 14722882]
126. Cunningham D, Lawton J, Jarra W, Preiser P, Langhorne J. The pir multigene family of *Plasmodium*: antigenic variation and beyond. Mol Biochem Parasitol. 2010; 170(2):65–73. [PubMed: 20045030]
127. Dasari P, Heber SD, Beisele M, Torzewski M, Reifenberg K, Orning C, Fries A, Zapf AL, Baumeister S, Lingelbach K, Udomsangpetch R, Bhakdi SC, Reiss K, Bhakdi S. Digestive vacuole of *Plasmodium falciparum* released during erythrocyte rupture dually activates complement and coagulation. Blood. 2012; 119(18):4301–10. [PubMed: 22403252]
128. Spaccapelo R, Janse CJ, Caterbi S, Franke-Fayard B, Bonilla JA, Syphard LM, Di Cristina M, Dottorini T, Savarino A, Cassone A, Bistoni F, Waters AP, Dame JB, Crisanti A. Plasmepsin 4-deficient *Plasmodium berghei* are virulence attenuated and induce protective immunity against experimental malaria. Am J Pathol. 2010; 176(1):205–17. [PubMed: 20019192]
129. Sun G, Chang WL, Li J, Berney SM, Kimpel D, van der Heyde HC. Inhibition of platelet adherence to brain microvasculature protects against severe *Plasmodium berghei* malaria. Infect Immun. 2003; 71(11):6553–61. [PubMed: 14573677]
130. van der Heyde HC, Gramaglia I, Sun G, Woods C. Platelet depletion by anti-CD41 (alphaIIb) mAb injection early but not late in the course of disease protects against *Plasmodium berghei* pathogenesis by altering the levels of pathogenic cytokines. Blood. 2005; 105(5):1956–63. [PubMed: 15494426]
131. Lamb TJ, Brown DE, Potocnik AJ, Langhorne J. Insights into the immunopathogenesis of malaria using mouse models. Expert Rev Mol Med. 2006; 8(6):1–22. [PubMed: 16556343]
132. Belnoue E, Kayibanda M, Vigario AM, Deschemin JC, van Rooijen N, Viguier M, Snounou G, Renia L. On the pathogenic role of brain-sequestered alphabeta CD8+ T cells in experimental cerebral malaria. J Immunol. 2002; 169(11):6369–75. [PubMed: 12444144]
133. Claser C, Malleret B, Gun SY, Wong AY, Chang ZW, Teo P, See PC, Howland SW, Ginhoux F, Renia L. CD8 T cells and IFN-gamma mediate the time-dependent accumulation of infected red blood cells in deep organs during experimental cerebral malaria. PLoS ONE. 2011; 6(4):e18720. [PubMed: 21494565]

134. Haque A, Best SE, Unosson K, Amante FH, de Labastida F, Anstey NM, Karupiah G, Smyth MJ, Heath WR, Engwerda CR. Granzyme B expression by CD8+ T cells is required for the development of experimental cerebral malaria. J Immunol. 2011; 186(11):6148–56. [PubMed: 21525386]

135. Nitcheu J, Bonduelle O, Combadiere C, Tefit M, Seilhean D, Mazier D, Combadiere B. Perforin-dependent brain-infiltrating cytotoxic CD8+ T lymphocytes mediate experimental cerebral malaria pathogenesis. J Immunol. 2003; 170(4):2221–8. [PubMed: 12574396]

136. Engwerda C, Belnoue E, Gruner AC, Renia L. Experimental models of cerebral malaria. Curr Top Microbiol Immunol. 2005; 297:103–43. [PubMed: 16265904]

137. Potchen MJ, Birbeck GL, Demarco JK, Kampondeni SD, Beare N, Molyneux ME, Taylor TE. Neuroimaging findings in children with retinopathy-confirmed cerebral malaria. Eur J Radiol. 2010; 74(1):262–8. [PubMed: 19345538]

138. Latourette MT, Siebert JE, Barto RJ Jr, Marable KL, Muyepa A, Hammond CA, Potchen MJ, Kampondeni SD, Taylor TE. Magnetic resonance imaging research in sub-Saharan Africa: challenges and satellite-based networking implementation. J Digit Imaging. 2011; 24(4):729–38. [PubMed: 20714916]

139. Hantson P, Hernalsteen D, Cosnard G. Reversible splenial lesion syndrome in cerebral malaria. J Neuroradiol. 2010; 37(4):243–6. [PubMed: 20381148]

140. Luvira V, Chamnanchanunt S, Thanachartwet V, Phumratanaprapin W, Viriyavejakul A. Cerebral venous sinus thrombosis in severe malaria. Southeast Asian J Trop Med Public Health. 2009; 40(5):893–7. [PubMed: 19842369]

141. Rasalkar DD, Paunipagar BK, Sanghvi D, Sonawane BD, Loniker P. Magnetic resonance imaging in cerebral malaria: a report of four cases. Br J Radiol. 2011; 84(1000):380–5. [PubMed: 21415303]

142. Nickerson JP, Tong KA, Raghavan R. Imaging cerebral malaria with a susceptibility-weighted MR sequence. AJNR Am J Neuroradiol. 2009; 30(6):e85–6. [PubMed: 19321625]

143. Kawai S, Sugiyama M. Imaging analysis of the brain in a primate model of cerebral malaria. Acta Trop. 2010; 114(3):152–6. [PubMed: 19467218]

144. Penet MF, Kober F, Confort-Gouny S, Le Fur Y, Dalmasso C, Coltel N, Liprandi A, Gulian JM, Grau GE, Cozzone PJ, Viola A. Magnetic resonance spectroscopy reveals an impaired brain metabolic profile in mice resistant to cerebral malaria infected with *Plasmodium berghei* ANKA. J Biol Chem. 2007; 282(19):14505–14. [PubMed: 17369263]

145. Dondorp AM, Ince C, Charunwatthana P, Hanson J, van Kuijen A, Faiz MA, Rahman MR, Hasan M, Bin Yunus E, Ghose A, Ruangveerayut R, Limmathurotsakul D, Mathura K, White NJ, Day NP. Direct *in vivo* assessment of microcirculatory dysfunction in severe falciparum malaria. J Infect Dis. 2008; 197(1):79–84. [PubMed: 18171289]

146. Siegenthaler N, Giraud R, Bendjelid K. Erythrocytapheresis and sublingual micro-vascular flow in severe malaria. Clin Hemorheol Microcirc. 2010; 46(4):299–304. [PubMed: 21187578]

147. De Backer D, Ospina-Tascon G, Salgado D, Favory R, Creteur J, Vincent JL. Monitoring the microcirculation in the critically ill patient: current methods and future approaches. Intensive Care Med. 2010; 36(11):1813–25. [PubMed: 20689916]

148. Patankar TF, Karnad DR, Shetty PG, Desai AP, Prasad SR. Adult cerebral malaria: prognostic importance of imaging findings and correlation with postmortem findings. Radiology. 2002; 224(3):811–6. [PubMed: 12202719]

149. Stevenson MM, Gros P, Olivier M, Fortin A, Serghides L. Cerebral malaria: human versus mouse studies. Trends Parasitol. 2010; 26(6):274–5. [PubMed: 20382077]

150. Hunt NH, Grau GE, Engwerda C, Barnum SR, van der Heyde H, Hansen DS, Schofield L, Golenser J. Murine cerebral malaria: the whole story. Trends Parasitol. 2010; 26(6):272–4. [PubMed: 20382078]

151. Riley EM, Couper KN, Helmby H, Hafalla JCR, de Souza JB, Langhorne J, Jarra WB, Zavala F. Neuropathogenesis of human and murine malaria. Trends Parasitol. 2010; 26(6):277–8. [PubMed: 20338809]

152. Frevert U, Movila A, Nikolskaia OV, Raper J, Mackey ZB, Abdulla M, McKerrow J, Grab DJ. Early invasion of brain parenchyma by African trypanosomes. PLoS One. 2012; 7(8):e43913. [PubMed: 22952808]
153. Holtmaat A, Bonhoeffer T, Chow DK, Chuckowree J, De Paola V, Hofer SB, Hubener M, Keck T, Knott G, Lee WCA, Mostany R, Mrsic-Flogel TD, Nedivi E, Portera-Cailliau C, Svoboda K, Trachtenberg JT, Wilbrecht L. Long-term, high-resolution imaging in the mouse neocortex through a chronic cranial window. Nat Protocols. 2009; 4(8):1128–44.
154. Yang G, Pan F, Parkhurst CN, Grutzendler J, Gan WB. Thinned-skull cranial window technique for long-term imaging of the cortex in live mice. Nat Protoc. 2010; 5(2):201–8. [PubMed: 20134419]
155. Dong, HW. The Allen Reference Atlas: A Digital Color Brain Atlas of the C57BL/6J Male Mouse. Seattle, WA: The Allen Institute for Brain Science. Wiley; 2008.
156. Fonager J, Franke-Fayard BM, Adams JH, Ramesar J, Klop O, Khan SM, Janse CJ, Waters AP. Development of the piggyBac transposable system for *Plasmodium berghei* and its application for random mutagenesis in malaria parasites. BMC Genomics. 2011; 12:155. [PubMed: 21418605]
157. Franke-Fayard B, Janse CJ, Cunha-Rodrigues M, Ramesar J, Buscher P, Que I, Lowik C, Voshol PJ, den Boer MA, van Duinen SG, Febbraio M, Mota MM, Waters AP. Murine malaria parasite sequestration: CD36 is the major receptor, but cerebral pathology is unlinked to sequestration. Proc Natl Acad Sci U S A. 2005; 102(32):11468–73. [PubMed: 16051702]
158. Suidan GL, McDole JR, Chen Y, Pirko I, Johnson AJ. Induction of blood brain barrier tight junction protein alterations by CD8 T cells. PLoS ONE. 2008; 3(8):e3037. [PubMed: 18725947]
159. von Zur Muhlen C, Sibson NR, Peter K, Campbell SJ, Wilainam P, Grau GE, Bode C, Choudhury RP, Anthony DC. A contrast agent recognizing activated platelets reveals murine cerebral malaria pathology undetectable by conventional MRI. J Clin Invest. 2008; 118(3):1198–207. [PubMed: 18274670]
160. Cabrales P, Zanini GM, Meays D, Frangos JA, Carvalho LJM. Murine cerebral malaria is associated with a vasospasm-like microcirculatory dysfunction, and survival upon rescue treatment is markedly increased by nimodipine. Am J Pathol. 2010; 176(3):1306–15. [PubMed: 20110412]
161. Lacerda-Queiroz N, Rodrigues DH, Vilela MC, Miranda ASd, Amaral DCG, Camargos ERdS, Carvalho LJdM, Howe CL, Teixeira MM, Teixeira AL. Inflammatory changes in the central nervous system are associated with behavioral impairment in *Plasmodium berghei* (strain ANKA)-infected mice. Exp Parasitol. 2010; 125(3):271–8. [PubMed: 20138873]
162. Amante FH, Haque A, Stanley AC, Rivera FdL, Randall LM, Wilson YA, Yeo G, Pieper C, Crabb BS, de Koning-Ward TF, Lundie RJ, Good MF, Pinzon-Charry A, Pearson MS, Duke MG, McManus DP, Loukas A, Hill GR, Engwerda CR. Immune-mediated mechanisms of parasite tissue sequestration during experimental cerebral malaria. J Immunol. 2010; 185(6): 3632–42. [PubMed: 20720206]
163. Baptista FG, Pamplona A, Pena AC, Mota MM, Pied S, Vigario AM. Accumulation of *Plasmodium berghei*-infected red blood cells in the brain is crucial for the development of cerebral malaria in mice. Infect Immun. 2010; 78(9):4033–9. [PubMed: 20605973]
164. Craig AG, Khairul MF, Patil PR. Cytoadherence and severe malaria. Malays J Med Sci. 2012; 19(2):5–18. [PubMed: 22973133]
165. Fonager J, Pasini EM, Braks JA, Klop O, Ramesar J, Remarque EJ, Vroegrijk IO, van Duinen SG, Thomas AW, Khan SM, Mann M, Kocken CH, Janse CJ, Franke-Fayard BM. Reduced CD36-dependent tissue sequestration of *Plasmodium*-infected erythrocytes is detrimental to malaria parasite growth in vivo. J Exp Med. 2012; 209(1):93–107. [PubMed: 22184632]
166. McAteer MA, Akhtar AM, von Zur Muhlen C, Choudhury RP. An approach to molecular imaging of atherosclerosis, thrombosis, and vascular inflammation using microparticles of iron oxide. Atherosclerosis. 2010; 209(1):18–27. [PubMed: 19883911]
167. McAteer MA, Choudhury RP. Chapter 4 - Applications of nanotechnology in molecular imaging of the brain. Prog Brain Res. 2009; 180:72–96. [PubMed: 20302829]

168. Carvalho-Tavares J, Hickey MJ, Hutchison J, Michaud J, Sutcliffe IT, Kubes P. A role for platelets and endothelial selectins in tumor necrosis factor-alpha-induced leukocyte recruitment in the brain microvasculature. Circ Res. 2000; 87(12):1141–8. [PubMed: 11110771]

169. Lacerda-Queiroz N, Lima OC, Carneiro CM, Vilela MC, Teixeira AL, Teixeira-Carvalho A, Araujo MS, Martins-Filho OA, Braga EM, Carvalho-Tavares J. *Plasmodium berghei* NK65 induces cerebral leukocyte recruitment in vivo: an intravital microscopic study. Acta Trop. 2011; 120(1-2):31–9. [PubMed: 21722620]

170. Owens T, Bechmann I, Engelhardt B. Perivascular spaces and the two steps to neuroinflammation. J Neuropathol Exp Neurol. 2008; 67(12):1113–21. [PubMed: 19018243]

171. McQuillan JA, Mitchell AJ, Ho YF, Combes V, Ball HJ, Golenser J, Grau GE, Hunt NH. Coincident parasite and CD8 T cell sequestration is required for development of experimental cerebral malaria. Int J Parasitol. 2011; 41(2):155–63. [PubMed: 20828575]

172. Haque A, Best SE, Amante FH, Mustafah S, Desbarrieres L, de Labastida F, Sparwasser T, Hill GR, Engwerda CR. CD4+ natural regulatory T cells prevent experimental cerebral malaria via CTLA-4 when expanded in vivo. PLoS Pathog. 2010; 6(12):e1001221. [PubMed: 21170302]

173. Fauconnier M, Palomo J, Bourigault ML, Meme S, Szeremeta F, Beloeil JC, Danneels A, Charron S, Rihet P, Ryffel B, Quesniaux VF. IL-12Rbeta2 is essential for the development of experimental cerebral malaria. J Immunol. 2012; 188(4):1905–14. [PubMed: 22238458]

174. Pino P, Vouldoukis I, Kolb JP, Mahmoudi N, Desportes-Livage I, Bricaire F, Danis M, Dugas B, Mazier D. *Plasmodium falciparum*--infected erythrocyte adhesion induces caspase activation and apoptosis in human endothelial cells. J Infect Dis. 2003; 187(8):1283–90. [PubMed: 12696008]

175. Jimenez B, Volpert OV, Crawford SE, Febbraio M, Silverstein RL, Bouck N. Signals leading to apoptosis-dependent inhibition of neovascularization by thrombospondin-1. Nat Med. 2000; 6(1): 41–8. [PubMed: 10613822]

176. Zougbede S, Miller F, Ravassard P, Rebollo A, Ciceron L, Couraud PO, Mazier D, Moreno A. Metabolic acidosis induced by *Plasmodium falciparum* intraerythrocytic stages alters blood-brain barrier integrity. J Cereb Blood Flow Metab. 2011; 31(2):514–26. [PubMed: 20683453]

177. Jambou R, Combes V, Jambou MJ, Weksler BB, Couraud PO, Grau GE. *Plasmodium falciparum* adhesion on human brain microvascular endothelial cells involves transmigration-like cup formation and induces opening of intercellular junctions. PLoS Pathog. 2010; 6(7):e1001021. [PubMed: 20686652]

178. Luissint AC, Artus C, Glacial F, Ganeshamoorthy K, Couraud PO. Tight junctions at the blood brain barrier: physiological architecture and disease-associated dysregulation. Fluids Barriers CNS. 2012; 9(1):23. [PubMed: 23140302]

179. Epiphanio S, Campos MG, Pamplona A, Carapau D, Pena AC, Ataide R, Monteiro CA, Felix N, Costa-Silva A, Marinho CR, Dias S, Mota MM. VEGF promotes malaria-associated acute lung injury in mice. PLoS Pathog. 2010; 6(5):e1000916. [PubMed: 20502682]

180. Suidan GL, Dickerson JW, Johnson HL, Chan TW, Pavelko KD, Pirko I, Seroogy KB, Johnson AJ. Preserved vascular integrity and enhanced survival following neuropilin-1 inhibition in a mouse model of CD8 T cell-initiated CNS vascular permeability. J Neuroinflammation. 2012; 9:218. [PubMed: 22985494]

181. Brinkmann V. FTY720 (fingolimod) in Multiple Sclerosis: therapeutic effects in the immune and the central nervous system. Br J Pharmacol. 2009; 158(5):1173–82. [PubMed: 19814729]

182. Brinkmann V, Billich A, Baumruker T, Heining P, Schmouder R, Francis G, Aradhye S, Burtin P. Fingolimod (FTY720): discovery and development of an oral drug to treat multiple sclerosis. Nat Rev Drug Discov. 2010; 9(11):883–97. [PubMed: 21031003]

183. Hla T, Brinkmann V. Sphingosine 1-phosphate (S1P): Physiology and the effects of S1P receptor modulation. Neurology. 2011; 76(8 Suppl 3):S3–8. [PubMed: 21339489]

184. Finney CA, Hawkes CA, Kain DC, Dhabangi A, Musoke C, Cserti-Gazdewich C, Oravecz T, Liles WC, Kain KC. S1P is associated with protection in human and experimental cerebral malaria. Mol Med. 2011; 17(7-8):717–25. [PubMed: 21556483]

185. Taylor PA, Ehrhardt MJ, Lees CJ, Tolar J, Weigel BJ, Panoskaltsis-Mortari A, Serody JS, Brinkmann V, Blazar BR. Insights into the mechanism of FTY720 and compatibility with

regulatory T cells for the inhibition of graft-versus-host disease (GVHD). Blood. 2007; 110(9): 3480–8. [PubMed: 17606761]

186. Idzko M, Hammad H, van Nimwegen M, Kool M, Muller T, Soullie T, Willart MA, Hijdra D, Hoogsteden HC, Lambrecht BN. Local application of FTY720 to the lung abrogates experimental asthma by altering dendritic cell function. J Clin Invest. 2006; 116(11):2935–44. [PubMed: 17080194]
187. Lee MJ, Thangada S, Claffey KP, Ancellin N, Liu CH, Kluk M, Volpi M, Sha'afi RI, Hla T. Vascular endothelial cell adherens junction assembly and morphogenesis induced by sphingosine-1-phosphate. Cell. 1999; 99(3):301–12. [PubMed: 10555146]
188. Chun J, Hartung HP. Mechanism of action of oral fingolimod (FTY720) in multiple sclerosis. Clin Neuropharmacol. 2010; 33(2):91–101. [PubMed: 20061941]
189. Dev KK, Mullershausen F, Mattes H, Kuhn RR, Bilbe G, Hoyer D, Mir A. Brain sphingosine-1-phosphate receptors: implication for FTY720 in the treatment of multiple sclerosis. Pharmacol Ther. 2008; 117(1):77–93. [PubMed: 17961662]
190. Haque A, Best SE, Amante FH, Ammerdorffer A, de Labastida F, Pereira T, Ramm GA, Engwerda CR. High parasite burdens cause liver damage in mice following *Plasmodium berghei* ANKA infection independently of CD8+ T cell-mediated immune pathology. Infect Immun. 2011; 79(5):1882–8. [PubMed: 21343349]
191. Lovegrove FE, Tangpukdee N, Opoka RO, Lafferty EI, Rajwans N, Hawkes M, Krudsood S, Looareesuwan S, John CC, Liles WC, Kain KC. Serum angiopoietin-1 and -2 levels discriminate cerebral malaria from uncomplicated malaria and predict clinical outcome in African children. PLoS ONE. 2009; 4(3):e4912. [PubMed: 19300530]
192. Conroy AL, Glover SJ, Hawkes M, Erdman LK, Seydel KB, Taylor TE, Molyneux ME, Kain KC. Angiopoietin-2 levels are associated with retinopathy and predict mortality in Malawian children with cerebral malaria: a retrospective case-control study. Crit Care Med. 2012; 40(3): 952–9. [PubMed: 22343839]
193. Conroy AL, Lafferty EI, Lovegrove FE, Krudsood S, Tangpukdee N, Liles WC, Kain KC. Whole blood angiopoietin-1 and -2 levels discriminate cerebral and severe (non-cerebral) malaria from uncomplicated malaria. Malar J. 2009; 8:295. [PubMed: 20003529]
194. Jain V, Lucchi NW, Wilson NO, Blackstock AJ, Nagpal AC, Joel PK, Singh MP, Udhayakumar V, Stiles JK, Singh N. Plasma levels of angiopoietin-1 and -2 predict cerebral malaria outcome in Central India. Malar J. 2011; 10:383. [PubMed: 22192385]
195. Kamiyama T, Tatsumi M, Matsubara J, Yamamoto K, Rubio Z, Cortes G, Fujii H. Manifestation of cerebral malaria-like symptoms in the WM/Ms rat infected with *Plasmodium berghei* strain NK65. J Parasitol. 1987; 73(6):1138–45. [PubMed: 2963898]
196. Handayani S, Chiu DT, Tjitra E, Kuo JS, Lampah D, Kenangalem E, Renia L, Snounou G, Price RN, Anstey NM, Russell B. High deformability of *Plasmodium vivax*-infected red blood cells under microfluidic conditions. J Infect Dis. 2009; 199(3):445–50. [PubMed: 19090777]
197. Vigario AM, Belnoue E, Cumano A, Marussig M, Miltgen F, Landau I, Mazier D, Gresser I, Renia L. Inhibition of *Plasmodium yoelii* blood-stage malaria by interferon alpha through the inhibition of the production of its target cell, the reticulocyte. Blood. 2001; 97(12):3966–71. [PubMed: 11389041]
198. Silamut K, Phu NH, Whitty C, Turner GD, Louwrier K, Mai NT, Simpson JA, Hien TT, White NJ. A quantitative analysis of the microvascular sequestration of malaria parasites in the human brain. Am J Pathol. 1999; 155(2):395–410. [PubMed: 10433933]
199. Griffiths M, Neal JW, Gasque P. Innate immunity and protective neuroinflammation: new emphasis on the role of neuroimmune regulatory proteins. Int Rev Neurobiol. 2007; 82:29–55. [PubMed: 17678954]
200. Lloyd KL, Kubes P. GPI-linked endothelial CD14 contributes to the detection of LPS. Am J Physiol Heart Circ Physiol. 2006; 291(1):H473–81. [PubMed: 16443672]
201. Zhou H, Andonegui G, Wong CH, Kubes P. Role of endothelial TLR4 for neutrophil recruitment into central nervous system microvessels in systemic inflammation. J Immunol. 2009; 183(8): 5244–50. [PubMed: 19786543]

202. Zhou H, Lapointe BM, Clark SR, Zbytnuik L, Kubes P. A requirement for microglial TLR4 in leukocyte recruitment into brain in response to lipopolysaccharide. J Immunol. 2006; 177(11): 8103–10. [PubMed: 17114485]

203. Jindal SK, Aggarwal AN, Gupta D. Adult respiratory distress syndrome in the tropics. Clin Chest Med. 2002; 23(2):445–55. [PubMed: 12092038]

204. Schraufnagel DE, Malik R, Goel V, Ohara N, Chang SW. Lung capillary changes in hepatic cirrhosis in rats. Am J Physiol. 1997; 272(1 Pt 1):L139–47. [PubMed: 9038913]

205. Wisse E, Zanger RB, Charels K, Smissen P, McCuskey RS. The liver sieve: considerations concerning the structure and function of endothelial fenestrae, the sinusoidal wall and the space of Disse. Hepatology. 1985; 5:683–692. [PubMed: 3926620]

206. Conhaim RL, Rodenkirch LA. Functional diameters of alveolar microvessels at high lung volume in zone II. J Appl Physiol. 1998; 85(1):47–52. [PubMed: 9655754]

207. Conhaim RL, Rodenkirch LA. Estimated functional diameter of alveolar septal microvessels in zone 1. Am J Physiol. 1996; 271(3 Pt 2):H996–1003. [PubMed: 8853334]

208. Ware LB, Matthay MA. The acute respiratory distress syndrome. N Engl J Med. 2000; 342(18): 1334–49. [PubMed: 10793167]

209. Maniatis NA, Kotanidou A, Catravas JD, Orfanos SE. Endothelial pathomechanisms in acute lung injury. Vascul Pharmacol. 2008; 49(4-6):119–33. [PubMed: 18722553]

210. Matute-Bello G, Frevert CW, Martin TR. Animal models of acute lung injury. Am J Physiol Lung Cell Mol Physiol. 2008; 295(3):L379–99. [PubMed: 18621912]

211. Aldridge AJ. Role of the neutrophil in septic shock and the adult respiratory distress syndrome. Eur J Surg. 2002; 168(4):204–14. [PubMed: 12440757]

212. Bux J, Sachs UJ. The pathogenesis of transfusion-related acute lung injury (TRALI). Br J Haematol. 2007; 136(6):788–99. [PubMed: 17341264]

213. Hasleton PS, Roberts TE. Adult respiratory distress syndrome - an update. Histopathology. 1999; 34(4):285–94. [PubMed: 10231395]

214. Worthen GS, Schwab B 3rd, Elson EL, Downey GP. Mechanics of stimulated neutrophils: cell stiffening induces retention in capillaries. Science. 1989; 245(4914):183–6. [PubMed: 2749255]

215. Doerschuk CM, Beyers N, Coxson HO, Wiggs B, Hogg JC. Comparison of neutrophil and capillary diameters and their relation to neutrophil sequestration in the lung. J Appl Physiol. 1993; 74(6):3040–5. [PubMed: 8366005]

216. O'Dea KP, Wilson MR, Dokpesi JO, Wakabayashi K, Tatton L, van Rooijen N, Takata M. Mobilization and margination of bone marrow Gr-1 high monocytes during subclinical endotoxemia predisposes the lungs toward acute injury. J Immunol. 2009; 182(2):1155–66. [PubMed: 19124759]

217. Cross LJ, Matthay MA. Biomarkers in acute lung injury: insights into the pathogenesis of acute lung injury. Crit Care Clin. 2011; 27(2):355–77. [PubMed: 21440206]

218. Johnson ER, Matthay MA. Acute lung injury: epidemiology, pathogenesis, and treatment. J Aerosol Med Pulm Drug Deliv. 2010; 23(4):243–52. [PubMed: 20073554]

219. Valecha N, Pinto RG, Turner GD, Kumar A, Rodrigues S, Dubhashi NG, Rodrigues E, Banaulikar SS, Singh R, Dash AP, Baird JK. Histopathology of fatal respiratory distress caused by Plasmodium vivax malaria. Am J Trop Med Hyg. 2009; 81(5):758–62. [PubMed: 19861606]

220. Tan LK, Yacoub S, Scott S, Bhagani S, Jacobs M. Acute lung injury and other serious complications of Plasmodium vivax malaria. Lancet Infect Dis. 2008; 8(7):449–54. [PubMed: 18582837]

221. Genrich GL, Guarner J, Paddock CD, Shieh WJ, Greer PW, Barnwell JW, Zaki SR. Fatal malaria infection in travelers: novel immunohistochemical assays for the detection of *Plasmodium falciparum* in tissues and implications for pathogenesis. Am J Trop Med Hyg. 2007; 76(2):251–9. [PubMed: 17297032]

222. Anstey NM, Handojo T, Pain MC, Kenangalem E, Tjitra E, Price RN, Maguire GP. Lung injury in vivax malaria: pathophysiological evidence for pulmonary vascular sequestration and posttreatment alveolar-capillary inflammation. J Infect Dis. 2007; 195(4):589–96. [PubMed: 17230420]

223. Maguire GP, Handojo T, Pain MC, Kenangalem E, Price RN, Tjitra E, Anstey NM. Lung injury in uncomplicated and severe *falciparum* malaria: a longitudinal study in papua, Indonesia. J Infect Dis. 2005; 192(11):1966–74. [PubMed: 16267769]

224. Price L, Planche T, Rayner C, Krishna S. Acute respiratory distress syndrome in *Plasmodium vivax* malaria: case report and review of the literature. Trans R Soc Trop Med Hyg. 2007; 101(7): 655–9. [PubMed: 17433389]

225. Lomar AV, Vidal JE, Lomar FP, Barbas CV, de Matos GJ, Boulos M. Acute respiratory distress syndrome due to vivax malaria: case report and literature review. Braz J Infect Dis. 2005; 9(5): 425–30. [PubMed: 16410895]

226. Rojo-Marcos G, Cuadros-Gonzalez J, Mesa-Latorre JM, Culebras-Lopez AM, de Pablo-Sanchez R. Acute respiratory distress syndrome in a case of *Plasmodium ovale* malaria. Am J Trop Med Hyg. 2008; 79(3):391–3. [PubMed: 18784231]

227. Taylor WR, Hanson J, Turner GD, White NJ, Dondorp AM. Respiratory manifestations of malaria. Chest. 2012; 142(2):492–505. [PubMed: 22871759]

228. Matthay MA. Conference summary: acute lung injury. Chest. 1999; 116(1 Suppl):119S–126S. [PubMed: 10424631]

229. Luh SP, Chiang CH. Acute lung injury/acute respiratory distress syndrome (ALI/ARDS): the mechanism, present strategies and future perspectives of therapies. J Zhejiang Univ Sci B. 2007; 8(1):60–9. [PubMed: 17173364]

230. Matthay MA, Zemans RL. The acute respiratory distress syndrome: pathogenesis and treatment. Annu Rev Pathol. 2011; 6:147–63. [PubMed: 20936936]

231. Mohan A, Sharma SK, Bollineni S. Acute lung injury and acute respiratory distress syndrome in malaria. J Vector Borne Dis. 2008; 45(3):179–93. [PubMed: 18807374]

232. Chopra M, Reuben JS, Sharma AC. Acute lung injury:apoptosis and signaling mechanisms. Exp Biol Med (Maywood). 2009; 234(4):361–71. [PubMed: 19176873]

233. Grommes J, Soehnlein O. Contribution of neutrophils to acute lung injury. Mol Med. 2011; 17(3-4):293–307. [PubMed: 21046059]

234. Anstey NM, Jacups SP, Cain T, Pearson T, Ziesing PJ, Fisher DA, Currie BJ, Marks PJ, Maguire GP. Pulmonary manifestations of uncomplicated *falciparum* and *vivax* malaria: cough, small airways obstruction, impaired gas transfer, and increased pulmonary phagocytic activity. J Infect Dis. 2002; 185(9):1326–34. [PubMed: 12001051]

235. Anstey NM, Russell B, Yeo TW, Price RN. The pathophysiology of vivax malaria. Trends Parasitol. 2009; 25(5):220–7. [PubMed: 19349210]

236. Serghides L, Smith TG, Patel SN, Kain KC. CD36 and malaria: friends or foes? Trends Parasitol. 2003; 19(10):461–9. [PubMed: 14519584]

237. Lovegrove FE, Gharib SA, Pena-Castillo L, Patel SN, Ruzinski JT, Hughes TR, Liles WC, Kain KC. Parasite burden and CD36-mediated sequestration are determinants of acute lung injury in an experimental malaria model. PLoS Pathog. 2008; 4(5):e1000068. [PubMed: 18483551]

238. Senaldi G, Vesin C, Chang R, Grau GE, Piguet PF. Role of polymorphonuclear neutrophil leukocytes and their integrin CD11a (LFA-1) in the pathogenesis of severe murine malaria. Infect Immun. 1994; 62:1144–1149. [PubMed: 8132319]

239. Carvalho LJ, Lenzi HL, Pelajo-Machado M, Oliveira DN, Daniel-Ribeiro CT, Ferreira-da-Cruz MF. *Plasmodium berghei*: cerebral malaria in CBA mice is not clearly related to plasma TNF levels or intensity of histopathological changes. Exp Parasitol. 2000; 95(1):1–7. [PubMed: 10864512]

240. Helegbe GK, Yanagi T, Senba M, Huy NT, Shuaibu MN, Yamazaki A, Kikuchi M, Yasunami M, Hirayama K. Histopathological studies in two strains of semi-immune mice infected with Plasmodium berghei ANKA after chronic exposure. Parasitol Res. 2011; 108(4):807–14. [PubMed: 20978790]

241. Fu Y, Ding Y, Zhou TL, Ou QY, Xu WY. Comparative histopathology of mice infected with the 17XL and 17XNL strains of *Plasmodium yoelii*. J Parasitol. 2012; 98(2):310–5. [PubMed: 22017443]

242. Hee L, Dinudom A, Mitchell AJ, Grau GE, Cook DI, Hunt NH, Ball HJ. Reduced activity of the epithelial sodium channel in malaria-induced pulmonary oedema in mice. Int J Parasitol. 2011; 41(1):81–8. [PubMed: 20816846]

243. Van den Steen PE, Geurts N, Deroost K, Van Aelst I, Verhenne S, Heremans H, Van Damme J, Opdenakker G. Immunopathology and dexamethasone therapy in a new model for malaria-associated acute respiratory distress syndrome. Am J Respir Crit Care Med. 2010; 181(9):957–68. [PubMed: 20093644]

244. Pena AC, Penacho N, Mancio-Silva L, Neres R, Seixas JD, Fernandes AC, Romao CC, Mota MM, Bernardes GJ, Pamplona A. A novel carbon monoxide-releasing molecule fully protects mice from severe malaria. Antimicrob Agents Chemother. 2012; 56(3):1281–90. [PubMed: 22155828]

245. Franke-Fayard B, Fonager J, Braks A, Khan SM, Janse CJ. Sequestration and tissue accumulation of human malaria parasites: can we learn anything from rodent models of malaria? PLoS Pathog. 2010; 6(9):e1001032. [PubMed: 20941396]

246. Patel SN, Serghides L, Smith TG, Febbraio M, Silverstein RL, Kurtz TW, Pravenec M, Kain KC. CD36 mediates the phagocytosis of *Plasmodium falciparum*-infected erythrocytes by rodent macrophages. J Infect Dis. 2004; 189(2):204–13. [PubMed: 14722884]

247. McCarter SD, Mei SH, Lai PF, Zhang QW, Parker CH, Suen RS, Hood RD, Zhao YD, Deng Y, Han RN, Dumont DJ, Stewart DJ. Cell-based angiopoietin-1 gene therapy for acute lung injury. Am J Respir Crit Care Med. 2007; 175(10):1014–26. [PubMed: 17322110]

248. Thurston G, Rudge JS, Ioffe E, Zhou H, Ross L, Croll SD, Glazer N, Holash J, McDonald DM, Yancopoulos GD. Angiopoietin-1 protects the adult vasculature against plasma leakage. Nat Med. 2000; 6(4):460–3. [PubMed: 10742156]

249. Karmpaliotis D, Kosmidou I, Ingenito EP, Hong K, Malhotra A, Sunday ME, Haley KJ. Angiogenic growth factors in the pathophysiology of a murine model of acute lung injury. Am J Physiol Lung Cell Mol Physiol. 2002; 283(3):L585–95. [PubMed: 12169578]

250. Kosmidou I, Karmpaliotis D, Kirtane AJ, Barron HV, Gibson CM. Vascular endothelial growth factors in pulmonary edema: an update. J Thromb Thrombolysis. 2008; 25(3):259–64. [PubMed: 17554593]

251. Corada M, Mariotti M, Thurston G, Smith K, Kunkel R, Brockhaus M, Lampugnani MG, Martin-Padura I, Stoppacciaro A, Ruco L, McDonald DM, Ward PA, Dejana E. Vascular endothelial-cadherin is an important determinant of microvascular integrity in vivo. Proc Natl Acad Sci U S A. 1999; 96(17):9815–20. [PubMed: 10449777]

252. Kaner RJ, Ladetto JV, Singh R, Fukuda N, Matthay MA, Crystal RG. Lung overexpression of the vascular endothelial growth factor gene induces pulmonary edema. Am J Respir Cell Mol Biol. 2000; 22(6):657–64. [PubMed: 10837361]

253. Ware LB, Kaner RJ, Crystal RG, Schane R, Trivedi NN, McAuley D, Matthay MA. VEGF levels in the alveolar compartment do not distinguish between ARDS and hydrostatic pulmonary oedema. Eur Respir J. 2005; 26(1):101–5. [PubMed: 15994395]

254. St Croix CM, Leelavanichkul K, Watkins SC. Intravital fluorescence microscopy in pulmonary research. Adv Drug Deliv Rev. 2006; 58(7):834–40. [PubMed: 16996641]

255. Lim LH, Bochner BS, Wagner EM. Leukocyte recruitment in the airways: an intravital microscopic study of rat tracheal microcirculation. Am J Physiol Lung Cell Mol Physiol. 2002; 282(5):L959–67. [PubMed: 11943660]

256. Jaryszak EM, Baumgartner WA Jr, Peterson AJ, Presson RG Jr, Glenny RW, Wagner WW Jr. Selected contribution: measuring the response time of pulmonary capillary recruitment to sudden flow changes. J Appl Physiol. 2000; 89(3):1233–8. [PubMed: 10956374]

257. Al-Mehdi AB, Tozawa K, Fisher AB, Shientag L, Lee A, Muschel RJ. Intravascular origin of metastasis from the proliferation of endothelium-attached tumor cells: a new model for metastasis. Nat Med. 2000; 6(1):100–2. [PubMed: 10613833]

258. Wagner WW Jr. Pulmonary microcirculatory observations in vivo under physiological conditions. J Appl Physiol. 1969; 26(3):375–7. [PubMed: 5773180]

259. Lien DC, Wagner WW Jr, Capen RL, Haslett C, Hanson WL, Hofmeister SE, Henson PM, Worthen GS. Physiological neutrophil sequestration in the lung: visual evidence for localization in capillaries. J Appl Physiol. 1987; 62(3):1236–43. [PubMed: 3106311]

260. Wagner WW Jr, Latham LP, Gillespie MN, Guenther JP, Capen RL. Direct measurement of pulmonary capillary transit times. Science. 1982; 218(4570):379–81. [PubMed: 7123237]

261. Kuhnle GE, Leipfinger FH, Goetz AE. Measurement of microhemodynamics in the ventilated rabbit lung by intravital fluorescence microscopy. J Appl Physiol. 1993; 74(3):1462–71. [PubMed: 8482691]

262. Lamm WJ, Bernard SL, Wagner WW Jr, Glenny RW. Intravital microscopic observations of 15-microm microspheres lodging in the pulmonary microcirculation. J Appl Physiol. 2005; 98(6): 2242–8. [PubMed: 15705726]

263. McCormack DG, Mehta S, Tyml K, Scott JA, Potter R, Rohan M. Pulmonary microvascular changes during sepsis: evaluation using intravital videomicroscopy. Microvasc Res. 2000; 60(2): 131–40. [PubMed: 10964587]

264. Fingar VH, Taber SW, Wieman TJ. A new model for the study of pulmonary microcirculation: determination of pulmonary edema in rats. J Surg Res. 1994; 57(3):385–93. [PubMed: 8072287]

265. Schneider P, Foitzik T, Kahrau S, Podufal A, Buhr HJ. An experimental rat model for studying pulmonary microcirculation by in vivo videomicroscopy. Microvasc Res. 2001; 62(3):421–34. [PubMed: 11678644]

266. Kuebler WM, Parthasarathi K, Lindert J, Bhattacharya J. Real-time lung microscopy. J Appl Physiol. 2007; 102(3):1255–64. [PubMed: 17095639]

267. Tabuchi A, Mertens M, Kuppe H, Pries AR, Kuebler WM. Intravital microscopy of the murine pulmonary microcirculation. J Appl Physiol. 2008; 104(2):338–46. [PubMed: 18006870]

268. Funakoshi N, Onizuka M, Yanagi K, Ohshima N, Tomoyasu M, Sato Y, Yamamoto T, Ishikawa S, Mitsui T. A new model of lung metastasis for intravital studies. Microvasc Res. 2000; 59(3): 361–7. [PubMed: 10792967]

269. Cortez-Retamozo V, Swirski FK, Waterman P, Yuan H, Figueiredo JL, Newton AP, Upadhyay R, Vinegoni C, Kohler R, Blois J, Smith A, Nahrendorf M, Josephson L, Weissleder R, Pittet MJ. Real-time assessment of inflammation and treatment response in a mouse model of allergic airway inflammation. J Clin Invest. 2008; 118(12):4058–66. [PubMed: 19033674]

270. Alencar H, Mahmood U, Kawano Y, Hirata T, Weissleder R. Novel multiwavelength microscopic scanner for mouse imaging. Neoplasia. 2005; 7(11):977–83. [PubMed: 16331883]

271. Bullen A. Microscopic imaging techniques for drug discovery. Nat Rev Drug Discov. 2008; 7(1): 54–67. [PubMed: 18079755]

272. Wagner, R. Erlaeuterungstafeln zur Physiologie und Entwicklungsgeschichte 1839. Leipzig, Germany: Leopold Voss;

273. Weigert R. Welcome to IntraVital. IntraVital. 2012; 1(1):1.

274. Mwakingwe A, Ting LM, Hochman S, Chen J, Sinnis P, Kim K. Noninvasive real-time monitoring of liver-stage development of bioluminescent *Plasmodium* parasites. J Infect Dis. 2009; 200(9):1470–8. [PubMed: 19811100]

275. Braks J, Aime E, Spaccapelo R, Klop O, Janse CJ, Franke-Fayard B. Bioluminescence imaging of *P. berghei* schizont sequestration in rodents. Methods Mol Biol. 2013; 923:353–68. [PubMed: 22990791]

Abbreviations

ALI/ARDS	acute lung infection/acute respiratory distress syndrome
BAB	blood alveolar barrier
BBB	blood brain barrier
CM	cerebral malaria
ECM	experimental cerebral malaria

HCM	human cerebral malaria
IVM	intravital microscopy
IRR	intravital reflection recording
LS	liver stage
MRI	magnetic resonance imaging
PbA	*Plasmodium berghei* ANKA
PyXL	*Plasmodium yoelii* 17XL
PCV	postcapillary venule
RBC	red blood cell
iRBC	infected red blood cell
TJ	tight junction
wt	wild type

Highlights

- Intravital microscopy (IVM) provides insights into *Plasmodium*-host interactions
- IVM enables the study of parasite immunobiology in multiple organs
- IVM visualizes the behavior of CD8+ effector T cells in the liver of *Plasmodium* infected and immunized mice
- IVM explains the mechanism of vascular leakage during experimental cerebral malaria
- IVM is a valuable tool to monitor the pathogenesis of malarial acute lung injury

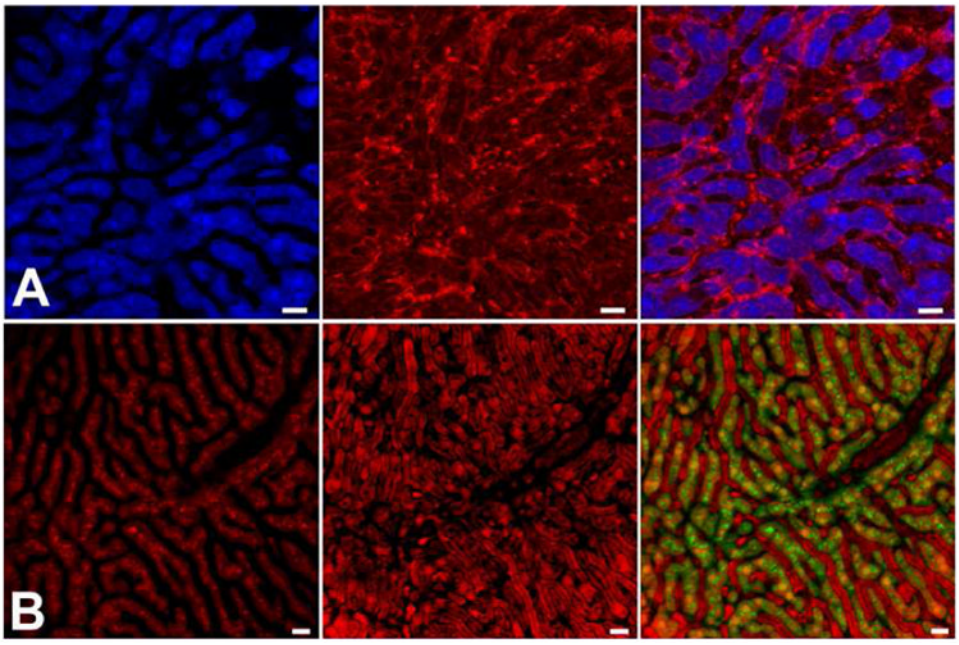

Figure 1. IRR enhances visualization of the sinusoidal blood flow

(a) Direct IRR visualizes blood cells traveling in the sinusoids (left panel). Fluorescence emission in this ECFP mouse liver (middle panel) is strongest in hepatocytes. Overlay of the two signals results in a complementary depiction of the non-fluorescent microvasculature and the fluorescent liver parenchyma (right panel). (b) Inverse IRR depicts blood cells traveling in the sinusoidal lumen as dark objects embedded in bright red plasma (left panel). Fluorescence in the DsRed mouse liver is most pronounced in hepatocytes (middle panel). Overlay of the inverse IRR and DsRed signals (pseudocolored in green) highlights the demarcation between hepatocytes and sinusoids (right panel). See [76] for details. Scale bars = 20 μm.

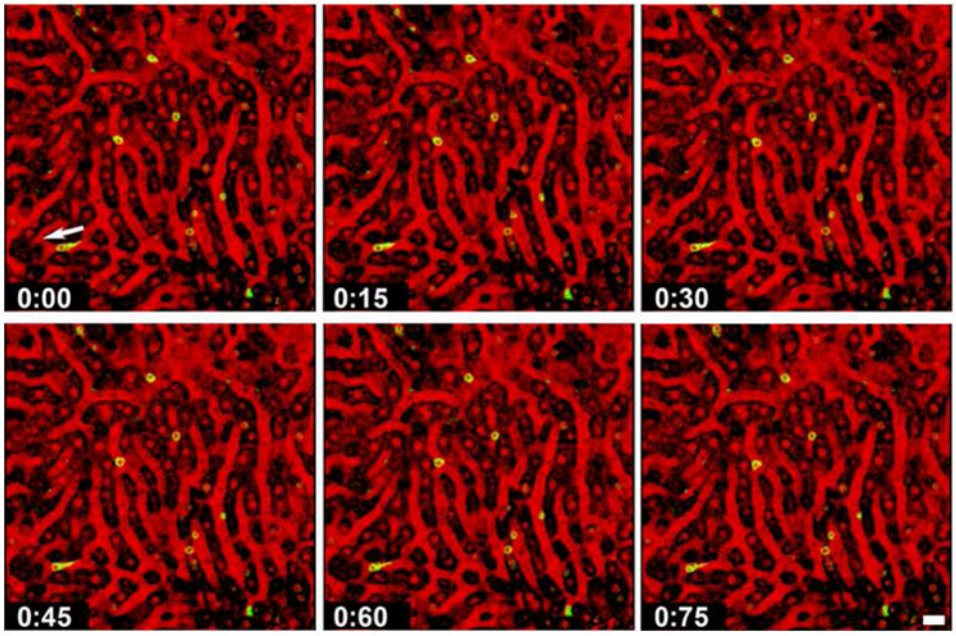

Figure 2. Visualizing the immunobiology of *Plasmodium* liver stages

Selected frames from a confocal IVM movie (see Video S1) showing CD8+ T cells (green) crawling slowly along the sinusoidal endothelium of a mouse liver. Note the trailing uropod of a CD8+ T cell, whose direction of movement is indicated by an arrow. Inverse IRR was used to visualize the architecture of this DsRed mouse liver. If direct IRR had been used, the non-fluorescent vascular lumen would have been dark and the blood cells, which reflect the laser light, would have appeared red. The hepatocyte cytoplasm of the DsRed mouse emits bright fluorescence and the nuclei are dim red. In inverse IRR mode (shown here), the sinusoidal lumen appears red and blood cells appear black. The hepatocyte cytoplasm appears dark and hepatocyte nuclei appear red. See [76] for details. Scale bar = 20 μm.

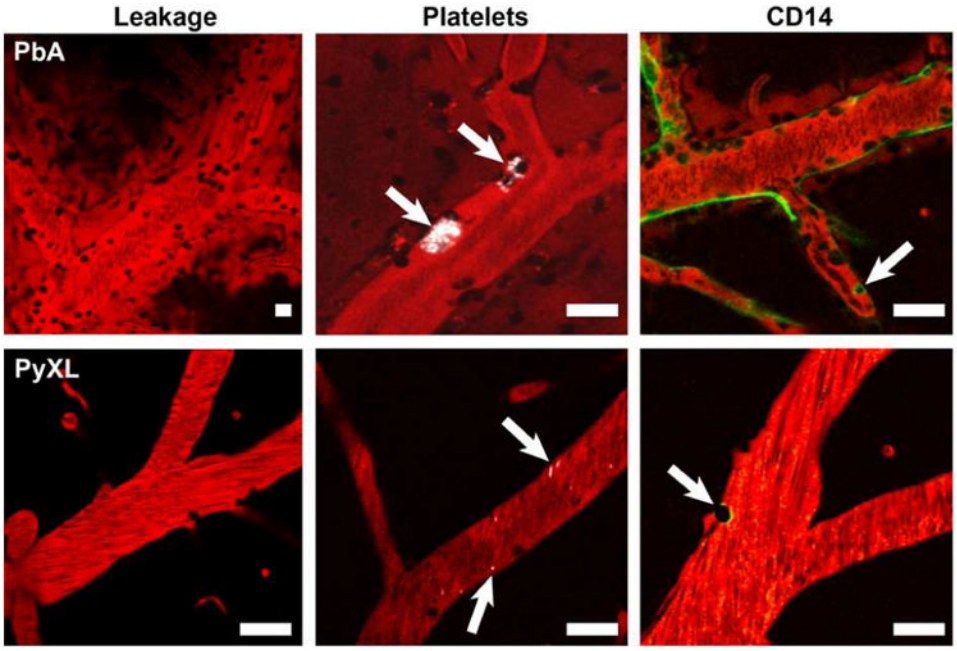

Figure 3. Imaging experimental cerebral malaria

During symptomatic ECM, PbA infected mice exhibit characteristic changes in PCV, but not capillaries or arterioles, including leakage of the plasma marker Evans blue (shown in red) into the perivascular space and the surrounding cerebral parenchyma, focal deposition of small aggregates of platelets (shown in white), appearance of the pattern recognition receptor CD14 on the luminal surface of the endothelium, and recruitment of various populations of leukocytes. Note the absence of vascular leakage, platelet deposition, and CD14 in PCV from PyXL infected mice with hyperparasitemia. Scale bars = 50 μm.

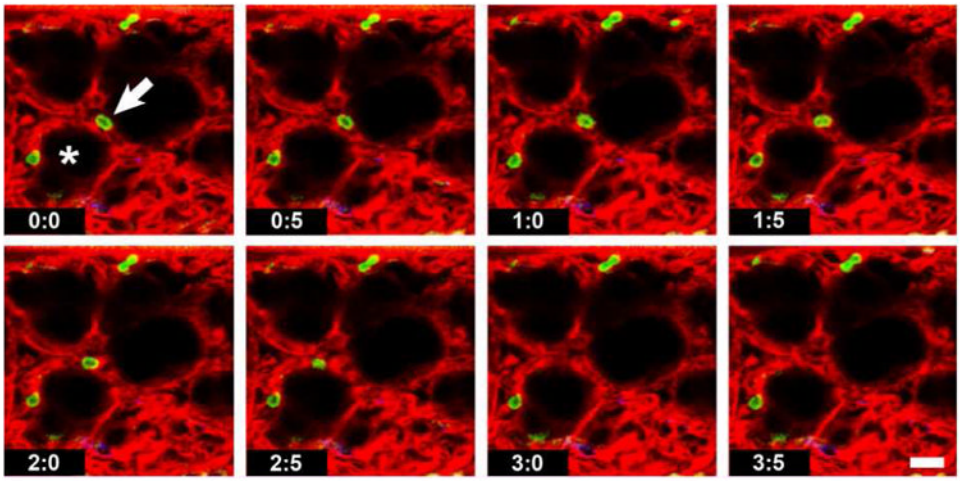

Figure 4. Intravital lung imaging

Consecutive frames from a movie of a live ventilated mouse lung. Synchronization of scan and respiratory rate allows image acquisition at the peak of every inspiration, which simulates immobilization of the lung surface. One of the Gr-1+ neutrophils (green) can be seen crawling along an alveolar capillary towards the left (arrow) until it disappears from view (at 3.0 s). The pulmonary microvasculature is visualized with Evans blue (red). The alveoli are inflated and appear black (asterisk). Scale bar = 20 μm.